CHAPTER VII

THE LARGE RADIO GALAXY CENTAURUS A

7.1 INTRODUCTION

The nearby galaxy Centaurus A (NGC5128) has always been an object of extensive optical, and radio studies. It is one of the five brightest galaxies in the sky ($m_V \sim 6$), and also the nearest galaxy having an active nucleus and associated with an extended double radio structure. Its distance has been recently re-estimated from the light curve of the supernova 1987g placing it at $\sim$ 3 Mpc (Frogel et al., 1987). The Elliptical (E2) image of this galaxy is bisected by a prominent lane of dust, gas and H II regions, extended roughly along a position angle of 126° (Baade and Minkowski, 1954). It is known to be a disk of diameter $\sim$ 15 kpc, thickness $\sim$ 1 kpc and having an inclination of $\sim 73^{\circ}$ to the plane of the sky (Graham, 1979; Dufour et al., 1979; Marcelin et al., 1982).

The association of Cen A with the powerful radio source was first established by Bolton et al. (1949). The radio source extends $\sim 10^{\circ}$ in the north-south, implying a size of $\sim$ 540 kpc, for the distance $D \sim 3$Mpc. The radio source shows several peaks in its structure, forming an overall S - shaped morphology (Haynes et al., 1983; Burns et al., 1983). This S shaped morphology is maintained even at size scales 2 orders of magnitude smaller, in the $\sim 7'$ arc double source (Maltby et al., 1963; Schwartz et al., 1973; Christiansen et al., 1977; Burns et al., 1983) which is embedded in the optical image of the galaxy (Fig.7.1a and 7.1b). The origin of this, remarkable S-shaped radio structure is investigated in this Chapter.

Faint, optical ripples or shell-like structures are known to be commonly associated with elliptical galaxies showing peculiar features (like tails, filaments, dust lanes) as well as those which are otherwise normal (Schweizer, 1980; Malin and Carter, 1983). Recently even spiral galaxies have been shown to possess such shell systems (Schweizer and Seitzer, 1988). Considering only ellipticals, shells are known to occur in ~10% of all bright elliptical galaxies (Quinn, 1984). There have been many observational and theoretical attempts to understand the formation of the shells (observational: Schweizer, 1980, 1983; Malin and Carter, 1980, 1983; Carter et al., 1982; Malin et al., 1983; Pence, 1986; Fort et al., 1986; Schweizer and Seitzer, 1988; Theoretical: Fabian et al., 1980; Quinn, 1982, 1984; Huang and Stewart, 1985; Williams and Christiansen, 1985; Kundt and Krause, 1985; Dupraz and Combes, 1986; Umemura and Ikeuchi, 1987).

Optical shells are sharply defined, arc-like features, not completely encircling the parent galaxy. They have been detected out to distances as large as ~ 200 kpc from the central galaxy, along the major axis, and as near as ~1 kpc from the galactic nucleus. One of their most characteristic properties is the inter-leaved disposition about the parent galaxy, i.e., the next outer shell occurs on the opposite side of the galaxy. Even the most sensitive optical observations carried out so far have failed to detect any emission lines. Their colours are seen to be bluer than, or similar to, those of the parent galaxy. From these results, it is has been been inferred that the shells are entirely made of stars. From photometric observations, it is deduced that the shells contain upto $\sim$ 10% of the mass of elliptical galaxy and contribute $\sim$ 0.5 - 5% of the total light. It has also been found that the shells occur mostly in galaxies located in sparsely populated environments (Quinn, 1984).

Among all the models for the shell formation the galaxy merger hypothesis first suggestd by Schweizer (1980) and later studied by several authors seems to account for most of observed properties of shells. Basically, in this model, the stars in different sections of the captured disk galaxy revolve about the centre of the $\sim$10 times more massive galaxy with different periods, because of their different energies. The inner-most sections have the shortest periods and form shells first. As the stars have their minimum velocities at the extremes of their oscillation, they spend most of their time at these extremities. The main deficiency of this model concerns the fate of the large amount of gas associated with the captured galaxy, in case it is a spiral.

The competing models for the shell formation, all involve interaction between an outflow from the parent galaxy and some external medium. Stars form, from the resulting density enhancements as they cool. These models are inadequate in accounting for the important shell properties like their interleaved distribution,their incomplete arc-like structure, and the same or somewhat bluer colours (of the stars in the shell) as those in the parent galaxy.

In the context of the model proposed in this chapter for explaining the S shaped radio structure of Cen A, two properties of the shells are important: their gas content and their rotation about the galactic nucleus. Neither of these properties has been ruled out by the merger scenario. So far only 2 shell velocities have been determined but it has not been possible to establish if the measured velocities are radial or circular relative to the nucleus (NGC3923; Quinn, 1982; NGC1316: Bosma et al., 1985).

Typical double radio galaxies, are more or less collinear. They may or may not contain emission peaks in their lobes. The C-shaped sources, WATs, HTs and NATs are all found in galaxy clusters. Like them, the S or Z shaped sources (eg. NGC315) too have been explained in terms of the continuous beam model. According to Henriksen et al. (1981), the twin jet would be refracted towards the galaxy minor axis (the direction of maximum pressure gradient), from their original direction of ejection. The S-shaped structure could also arise due to precession of the basic ejection axis itself (eg. for NGC326, Ekers et al., 1978). The model of Gopal-Krishna and Chitre (1983) explains the S-shaped structure in terms of an interaction of the jets with the shell segments rotating about the parent galaxy.

In the particular case of Cen A the S-shaped structure is delineated by discrete emission peaks, so any suggested model must also explain their origin. Haynes et al. (1983) proposed multiple nuclear outbursts along a precessing ejection axis.

The discovery and detailed studies of radio jets, which in some are seen connecting the nucleus all the way to the hotspots, posed difficulties for the discrete plasmon ejection models while providing all support for the continuous beam model. Moreover, if jets are interpreted as channels for the ejected plasmons, their centre brightened profiles indicative of emission from within them, imply that the channels are filled. The many numerical simulations of a bulk flow impinging upon an external medium successfully reproduced the observed powerful radio source morphologies (Norman et al., 1982). Again based on the continuous beam model, Gopal-Krishna and Wiita (1987) could account for the linear size evolution of powerful doubles.

The model for the S-shaped and multi-peaked radio structure seen in Cen A, that is presented here, does not need to do away with the continuous beam ejection scenario, and quite naturally accounts for the S shape of the discrete peaks (Gopal-Krishna and Saripalli, 1984b). Our study is based on a detailed comparison of recent deep optical and radio photographs of Cen A. It further allows us to place lower limit to the gas density in the optical shells, besides yielding constraints on the physical parameters of the jet. The shell is inferred to contain gas at significant levels, though its signature (emission lines) has not been directly detected despite several 1000 sec. of integration.

7.2 COMPARISON OF RADIO AND OPTICAL MAPS

Radio maps:

For the present study we make use of 3 radio maps of Cen A. The first is the Parkes map made at 1.4 GHz by Cooper et al. (1965) with a coarse angular resolution of 14' arc (Fig.7.1a). The new Parkes map of the source shown in Fig.7.1c has been made at 5 GHz with a 4' beam (Haynes et al., 1983). The third radio map shown in Fig.7.2a, covers only a small region, containing the inner double radio source and has been made by Schreier et al. (1981) using the VLA at 1.4 GHz with a resolution of 10" x 31" arc. From this map it can be seen that the extensions of the two inner lobes indicate an inversion symmetry about the central core, in the same clockwise sense as displayed by the outer radio peaks (Fig.7.1). The nuclear radio source is seen to be joined to the base of the northern inner lobe by a roughly collinear chain of radio/X-ray knots (Schreier et al., 1981; Fig.7.2; see also Brodie et al., 1983 for the optical knots in this region). From optical and radio depolarization studies (Dufour and van den Bergh, 1978; Graham and Price, 1981) it is known that the northern jet is likely to be approaching

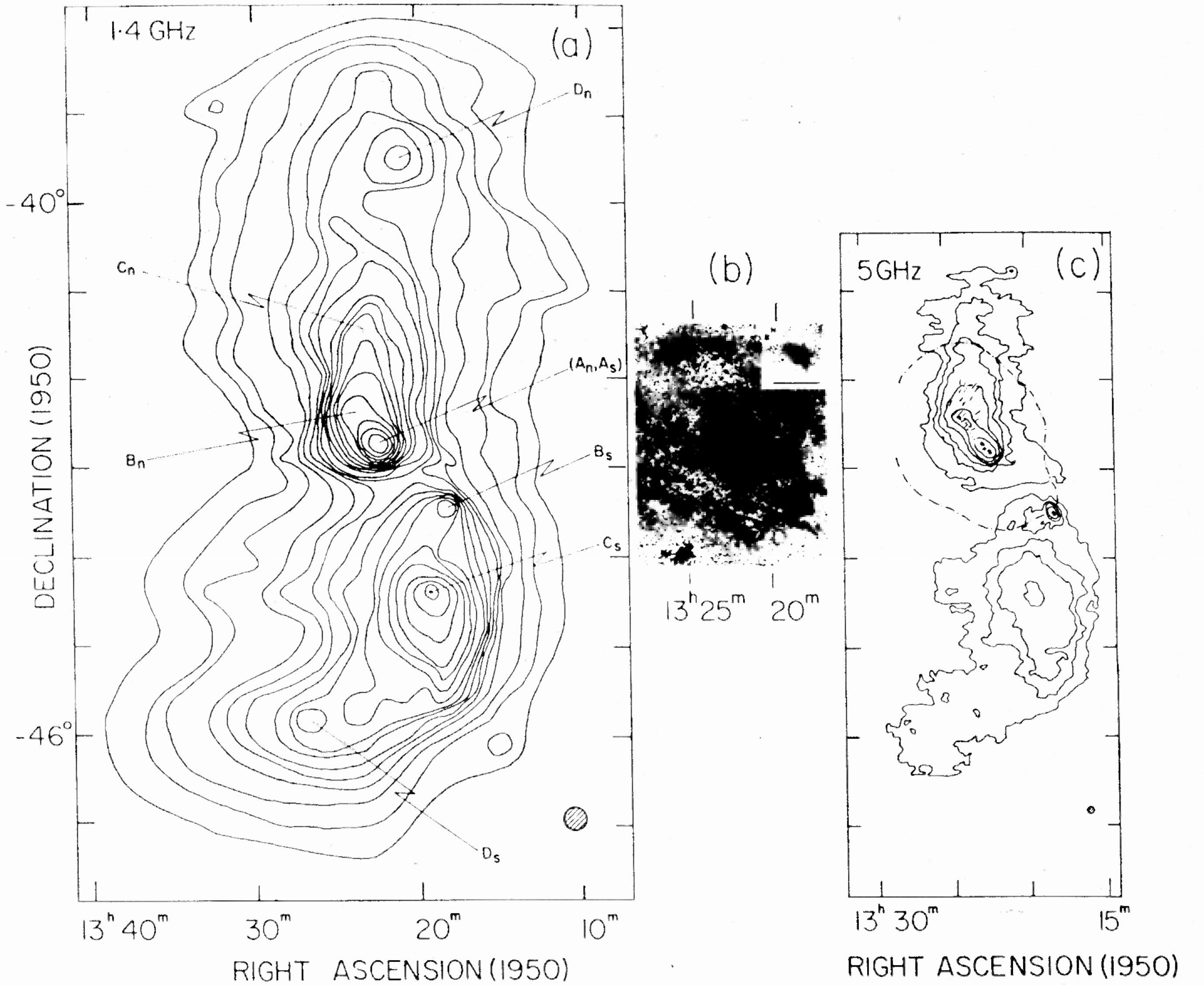

Fig. 7.1 a–c. Shown are three wide-field pictures of Cen A, all reduced to the same angular scale and aligned in declination. These are: **a** The Parkes 1.4 GHz map showing the two giant radio lobes of Cen A, stretched over ~ 10° (Cooper et al., 1965). The four northern radio peaks and their southern counterparts are marked as *A*, *B*, *C* and *D* (see text). Note the clockwise progression in the position angles of the successively outer pairs of radio peaks. The central peak marked as (A_N, A_S) is seen resolved into two peaks, A_N and A_S, in **c**. **b** A specially processed, high-contrast photograph covering a ~ 2° × 3° field around Cen A, reproduced from Malin (1978). The inset in the upper right corner shows a normally processed photograph of Cen A, the scale being the same as that of the main photograph. **c** The 5 GHz Parkes map of Cen A, reproduced from Haynes et al. (1983), after appropriately contracting their published map in east-west direction and thereby compensating for the expansion of the right ascension scale relative to the declination scale, as present on their map. The 'plus' mark near the centre refers to the position of the stellar nucleus of the galaxy, as defined by Kunkel and Bradt (1971). The dotted curve running northeast from the nucleus represents the outer parts of the optical jet, as published by Graham and Price (1981) (see text). The dashes plotted in the region of the radio lobe B_N indicate the orientation of magnetic field, as inferred from the linear polarization map made by Gardner and Whiteoak (1971) at 5 GHz. The dash-dotted curve is a schematic representation of the giant shell-type structure of radius ~ 1°, seen on the optical photograph in **b**, surrounding the main body of Cen A. The designations to the various radio peaks are given in **a**

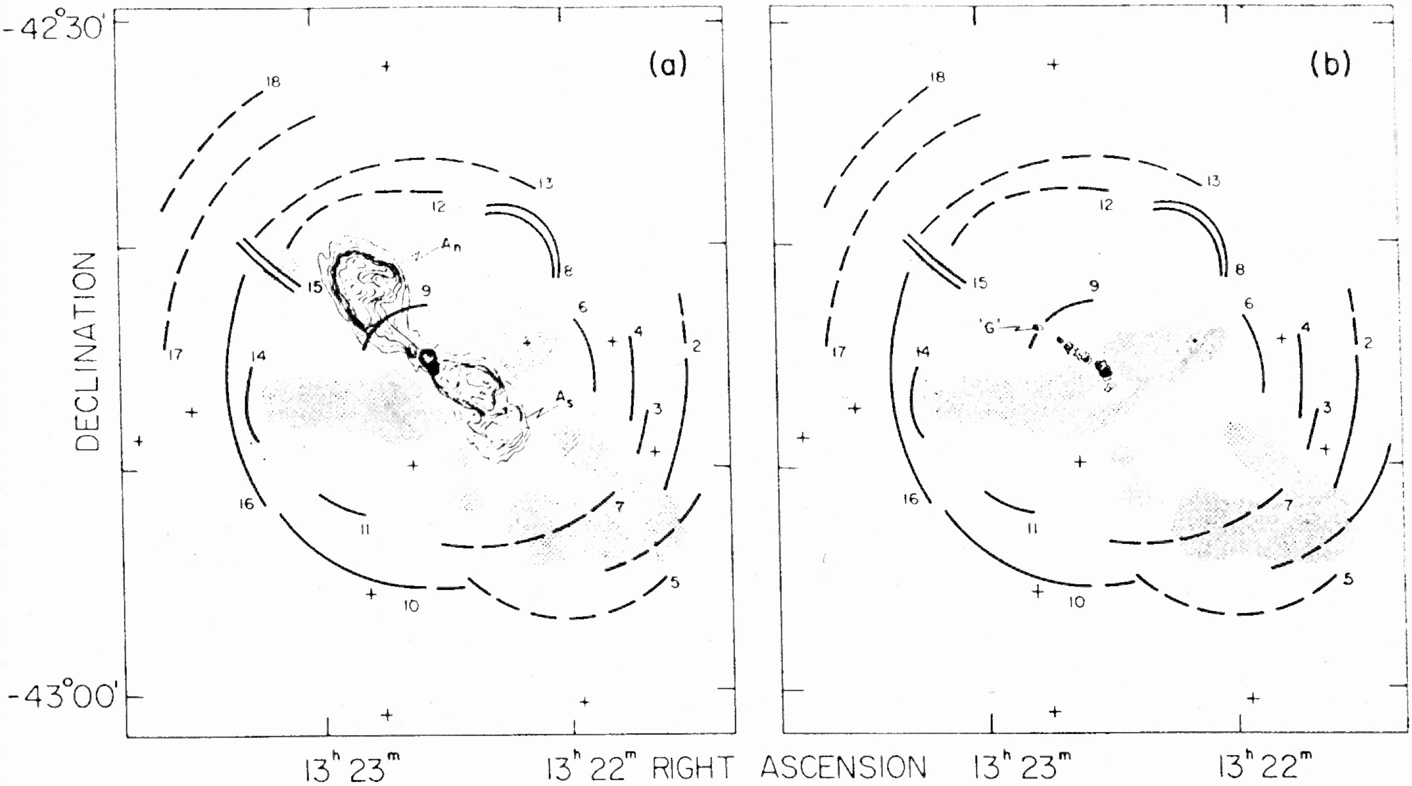

Fig.7.2 a The 1.4 GHz VLA map of the inner double source in Cen A (Schreier et al., 1981), superposed on the sketch of the optical features discovered recently in Cen A by Malin et al. (1983) and reproduced here from their paper. The shaded areas show absorption regions while the crosses indicate the positions of bright reference stars using which we have drawn the position coordinates. Full arcs represent the sharpest structures, broken arcs those more blurred. **b** same as **a** except that the radio map has been substituted with a high resolution, soft X-ray map published by Schreier et al. (1981). The X-ray peak coincident with the shell segment 9 has been designated as "*G*" by these authors

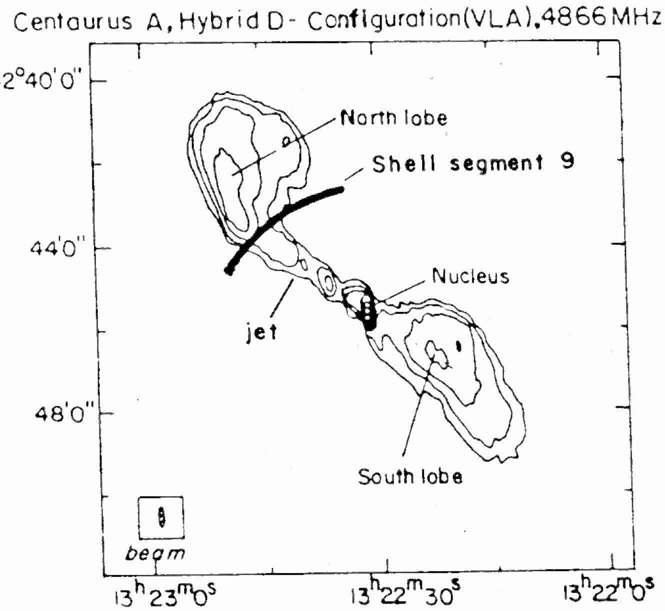

Fig.7.2(c) The optically detected shell segment 9, described by Malin et al. (1983), is superposed on the VLA 5 GHz map of the inner double radio source of Centaurus A, made by Burns et al. (1983). Absolute position of the shell segment was determined using the bright reference stars in its field, plotted by Malin et al.

us.

The optical photographs

For both the optical photographs that are used by us for the study, the dynamic range has been greatly enhanced by employing techniques of unsharp masking and photographic amplification (Malin, 1977). The first photograph shown in Fig.7.1b. covers $\sim 2^{\circ}x3^{\circ}$ field centred at Cen A (Malin, 1978). The image of the galaxy is seen to be extended by $\sim 1.2^{\circ}$ in PA $\sim 30^{\circ}$, in agreement with the earlier results from Johnson (1963). Also, a ring like feature with a radius of $\sim 1^{\circ}$ is seen to surround the galaxy. Its possible role in shaping the radio morphology of Cen A will be discussed below.

The second deep optical photograph (Malin et al., 1983) shows a system of shell segments within $\sim$ 20 kpc of the nucleus of Cen A These authors have provided a sketch of the shell segments observed in the photograph. This is reproduced in Fig.7.2. It can be seen that the shells are more regular on the north-eastern (NE) side. In the south-western (SW) side however detection of such shells may be hampered due to the presence of the dust lane. The feature marked 15, is a gaseous emission filament and is probably related to the optical jet extending up to the NE "Middle radio lobe" (marked B_N in Fig.7.1a; Blanco et al., 1975; Peterson et al., 1975; also see Fig.7.1c). According to Malin et al. (1983) most of the remaining features sketched in Fig.7.2 can be interpreted as being remnants of a smaller disk galaxy that merged into Cen A about 10^9 yrs ago. In their scheme, incorporating the model developed by Quinn (1982) the shell segments are expected to rotate in order to counter the gravitational pull of the central elliptical galaxy. We shall assume hereafter that the general sense of rotation is clockwise for all the optically detected shell segments seen around Cen A (Fig.7.1b and Fig.7.2). As will be seen below, this plausible assumption seems to lead to a consistent explanation for the rather complex radio morphology observed in this galaxy.

7.3 RESULTS AND DISCUSSION

In Fig.7.1, the four radio peaks B_N, A_N, A_S and B_S fall on a straight line passing through the nucleus of Cen A. One could therefore imagine them to represent the inner (A_N, A_S) and middle (B_N, B_S) radio lobe pairs. However in the past, the component B_S was believed to be unrelated to Cen A, and instead thought to be associated with a 15-mag background elliptical galaxy (Cooper et al., 1965; also Haynes et al., 1983). From the recent 5 GHz Parkes map (Fig.7.1c) whose absolute positional accuracy is believed to be better than 30" arc we measured the position of this peak B_S as: RA(1950)=$13^h18^m12.2^s \pm 1.5^s$ and Dec (1950) = $-43^\circ 28'15" \pm 20"$. A check with the SRC/ESO survey print reveals that the centre of the said 15-mag galaxy is displaced by $2'.1 \pm 0'.7$ from the radio peak B_S along PA 25°. Thus although part of the emission from B_S may be associated with the background elliptical it seems more natural to consider the peak B_S as the counter-part of B_N, particularly in view of its good alignment with the peaks B_N, A_N and A_S, and also considering its extension towards the nucleus (Fig.7.1c). We therefore interpret the radio peak B_S as having formed due to the impact of the counter-jet into the south western section of the giant optical shell surrounding Cen A. (see Fig.7.1b and 7.1c). This view is substantiated by the good spatial coincidence between the radio component B_S and the relevant section of the optical shell (Fig.7.1) and furthermore by the eastward radio extension of B_S, which could conceivably result from the sweeping of the jet fluid by the shell in clockwise rotation about the galaxy as mentioned above (Fig.7.1c).

A radio enhancement is similarly seen near the northern section of the giant optical shell close to Dec. = $-41^{\circ}40'$, and we pair this radio peak C_N with the peak C_s in the southern lobe (Fig.7.1). The outermost peak D_N could be clearly paired with the peak D_S. Although the deep optical photograph shown in Fig.7.1b is not extensive enough to cover the region of the radio peaks D_N, D_S and C_S, we suggest that these peaks too owe their existence to the presence of shells farther out from the nucleus (requiring them to be at a distance of ~ 200 kpc from the nucleus) but still embedded within the giant radio lobes. It can be mentioned here that optical shells have been seen to occur at distances of as much as 200 kpc from the parent galaxy (for NGC 3923; see Athanassoula and Bosma, 1985). This postulated scenario is substantiated by the interpretation given below for the formation of the inner double radio source. Presently, it can be noted that all the 4 pairs of radio peaks, as proposed in our scheme are reasonably well aligned with respect to the galactic nucleus their axes showing a systematic progression in position angle (Fig.7.1).

In Fig.7.2a we have superposed the contours of the inner radio double and the shell segments found embedded inside the main body of Cen A described earlier. The most remarkable aspect of this radio-optical comparison is the close coincidence of the shell segment 9 with the point from where onwards the jet outflow is no longer straight but begins to deflect towards northwest, accompanied by an abrupt rise in brightness and flaring in the transverse direction. It appears therefore that at this point the jet flow has been interrupted by the rotating shell (see below). The outermost X-ray knot detected in the jet of Cen A, designated as knot "G" by Schreier et al. (1981), also coincides with the shell, strengthening the case for the proposed collision of the jet with the shell segment 9 (Fig.7.2b). The bending of the jet is even more clearly visible on the 5 GHz map reproduced in Fig.7.2c from Burns et al. (1983).

If under the gravitational influence of the central galaxy, this shell segment is also rotating in the clockwise sense, as postulated by us for the general rotation field around the main body of Cen A, the northward bending of the jet, soon after its being interrupted by the shell 9, might have resulted due to the transverse momentum imparted by the shell medium to the jet fluid. Also the eastward extension observed in the SW inner radio lobe A_S may have arisen due to the counter-jet being interrupted by a possible southwestern counterpart of the shell 9, whose detection would be rendered difficult due to obscuration caused by the dust lane (Fig.7.2). Below, we shall explore the condition under which the postulated encounter with the shell 9 could have deflected the jet.

For the shell segment 9, the Keplerian rotational velocity would be $V_S = \{GMg(\theta)/R_S\}^{1/2} \simeq 413$ km S^{-1} at the observed separation $\theta \sim 3'$ arc from the nucleus (which corresponds to a physical separation $R_S = \theta . D \simeq 2.6$ Kpc for a distnace D = 3Mpc for Cen.A) and taking the galaxy mass to be $M_g(\theta) = 10^{11} M_\odot$ within the radius $\theta \sim 3'$ (Marcelin et al., 1982). In the case when the galactic mass is a few times higher as inferred from the recent analysis by Hesser et al. (1984), a value for $V_S \sim 645$ kmS^{-1} would be more appropriate. For the width of the shell 9 no good estimate is available presently. But from inspection of the photograph published by Malin et al. (1983), we estimate that the shell width d_S is unlikely to be smaller than the width of the jet which is $d_j = 2r_j \simeq 34''$ arc at the position where the jet appears to encounter the shell segment. Thus $(d_S/d_j) \geq 1$. The above estimate of d_j given by Burns et al. (1983) refers to the main jet which as found by these authors, is surrounded by a 2-3 times wider sheath of radio emission. The energy flux L_j flowing through the jet is estimated as follows: if the energy flux L_j through the jet carried in the form of kinetic energy of the jet fluid of density ρ_j is converted into radio emission inside the NE-inner lobe with a net efficiency ε , then

$$L_r = \pi r_j^2 v_j \gamma_j (\gamma_j - 1) \rho_j c^2 \varepsilon \left(\frac{r_j}{r_{lobe}} \right)^{2/3} \qquad \ldots(7.1)$$

where

L_r = observed radio luminosity of the N_E inner lobe

= $1.44.10^{40}$ erg s^{-1} (Burns et al., 1983)

v_j = bulk velocity of the jet fluid

γ_j = bulk Lorentz factor = $[1-(v_j/c)^2]^{-1/2}$,

$(r_j/r_{lobe})^{2/3}$ = 0.303 for $r_{lobe} = 6.r_j$ (Burns et al. 1983)

which is the factor accounting for the adiabatic expansions, and c = velocity of light.

The angle of deflection of the jet, ϕ due to the transverse pressure of the shell 9, can be expressed as the ratio of the momenta of the shell and the jet, given by,

$$\tan \phi = \frac{\rho_s \, v_s^2}{\gamma_j^2 \rho_j \, v_j^2} \left(\frac{d_s}{d_j} \right) \qquad \ldots(7.2)$$

From the equation (7.1) and (7.2), we obtained

$$\tan \phi = \frac{\pi \, \varepsilon d_j^2 \rho_s \, v_s^2 \, c^2}{4 \, L_r \, v_j} \left(\frac{\gamma_j - 1}{\gamma_j} \right) \left(\frac{d_s}{d_j} \right) \left(\frac{d_j}{d_{lobe}} \right)^{2/3} \qquad \ldots(7.3)$$

From this relation one can obtain a useful limit to the density of gas in the shell. The true angle of deflection of the jet plasma can be derived from the apparent angle of deflection $\eta \sim 40^\circ$ (Fig.7.2c) using the following expression from Readhead et al. (1980).

$$\eta = \tan^{-1}\left(\frac{\sin\phi\,\sin\psi}{\sin\theta\,\cos\phi + \cos\theta\,\sin\phi\,\cos\psi}\right) \qquad (7.4)$$

Here ψ is the angle between the plane containing the tangent at the origin of the jet and the line of sight, and the plane containing the longitudinal axis of the jet. θ is the angle of inclination of the jet from the line of sight.

Because of the nearness of Cen A, detailed kinematic studies of the dustlane have been possible which yielded a measure of the orientation of its rotation axis with respect to the line of sight of $73^\circ \pm 3^\circ$ (Graham, 1979; Marcelin et al., 1982). From studies of radio galaxies with jets and having dust lane in their parent galaxies (Kotanyi and Ekers, 1979; Ekers and Simkin, 1983) it has been inferred that the inner radio jet in Cen A, is likely to be within $\sim 20^\circ$ of the rotation axis of the dustlane. Thus the inclination angle of the jet from the line of sight, . is likely to be $\geq 53^\circ \pm 3^\circ$.

Now, the true angle of deflection ϕ would be minimised for

$$\psi = \tan^{-1}\left(\frac{-\cot\eta}{\cos\theta}\right)$$

For, $\eta \sim 40^{o}$ and $\theta \geq 50^{o}$, from Eq.(7.4), the true angle of deflection ϕ is atleast $\sim 30^{o}$.

From Eq.(7.3), therefore, using the values discussed above for the various parameters, we obtain, for the gas density in the shell

$$\rho_s > 9.6.\ 10^{-39}\ [\ \frac{V_j}{\varepsilon}\ (\ \frac{\gamma_j}{\gamma_j - 1}\ )\ ] \qquad ...(7.5)$$

For the limiting values of $V_j = c$ ($\gamma_j = \infty$) and $\epsilon = 1$ the right hand side approaches a minimum yielding

$$\rho_s > 2.9.10^{-28}\ \text{gm cm}^{-3}$$

Adopting more realistic values of $\epsilon \lesssim 0.3$ a gas density of $\rho_s \geq 1.0.10^{-27}$ gm cm^{-3} is obtained for the shell. This is the minimum gas density in the shell needed to deflect the jet plasma through the observed angle of $\sim 40^{o}$.

An Independent Estimate of the Lobe Magnetic Field

As seen from Fig.7.2, the shell 9 extends by $\alpha \sim 2'.8$ arc west of the point where the jet is currently seen to impinge on it. The clockwise rotation of the shell with the Keplerian velocity of $V_s \sim 413$ kms^{-1} (see above) would then imply that it began to interrupt the jet (thereby initiating the formation of the NE inner lobe) at a time τ ago, where, $\tau = \alpha D/V_s = 6.0.10^{6}$yr.

The apparent break in the radio spectrum of this lobe at $\nu_b \sim 5$ GHz (Fig.7.2 of Slee et al., 1983) may then have arisen owing to synchrotron losses in a magnetic field H given by $H = 10^8/(\tau^2\nu_b)^{1/3}$ G. Using the above estimate τ of $\sim 6.10^6$ yr we obtain H = 18.3 μG. This value of H is 2 times lower than the equipartition magnetic field of 39 μG estimated by minimising the internal energy (Feigelson et al., 1981). But our estimate is quite close to the field strength of 14 μG obtained by Burns et al. (1983) by minimizing the internal pressure due to relativistic particles and magnetic field. It may be noted that the deduced value of H is quite insensitive to uncertainties in the various parameters, excepting in the distance D which is fairly well known.

It may be mentioned here that recently in the numerical simulation studies of jet disruption caused by shocks (Norman et al., 1988), the morphology of the northern lobe of the inner double in Cen A was reproduced via an oblique shock at the end of the jet. In this picture, the hypothetical oblique shock replaces the observed shell segment used in our explanation. However, the possibility of the observed optical emission (non synchrotron) in such shocks remains to be demonstrated. Moreover the idea of the twin jets interacting with the rotating shell segments naturally explains the S-shaped structure of the inner double.

The postulated interruption of the jet outflow at the shell segment 9 for the past $\sim 10^7$ yr is consistent with the conspicuous lack of radio emission between the radio peak A_S

and the next peak B_N (Fig.7.1a; 7.1c). The relativistic particles that had already advanced beyond the location into which the rotating shell segment subsequently moved in (and thus began to interrupt the jet flow) have, in the meanwhile, continued to advance further into the region of the radio peak B_N and possibly further out, thus creating an emission trough between A_N and B_N. The lack of radio emission just beyond A_N (the NE inner lobe) is seen clearly on the VLA map (Fig.7.2a). In Fig.7.1c, the dotted curve drawn near the central region marks the location of several optical emission features and dust patches observed out to about 25' arc from the nucleus (as described e.g., by Blanco et al., 1975; Graham and Price, 1981). Within $\sim$ 4' arc NE of the nucleus, i.e., in the region where the jet is almost straight and discernible in radio and X-rays, the optical filaments appear to line up along the jet (Brodie et al., 1983; Dufour and van den Bergh, 1978), but subsequently their chain gradually bends clockwise, ending up in the region of the radio component B_N (Fig.7.1c; 7.1a). It has been suggested by several authors that the formation of these filaments lying close to the trajectory of the jet has been triggered due to compression produced by the passage of the jet material in past (e.g.,Osmer, 1978; Graham, 1983; see also DeYoung,1981).

The gradual clockwise bending of the optical jet between the peaks A_N and B_N, as described above, could again be understood within the framework of the postulated clockwise rotation of the circumgalactic medium. But the rather abrupt bending towards north, exhibited by the radio contours just beyond the peak B_N seems more difficult to comprehend (Fig.7.1c; 7.1a). This is particularly so because the region of the abrupt bend seems to be devoid of any conspicuous, sharp optical feature like a shell segment (Fig.7.1; see also Fig.4 of Haynes et al., 1983). Nonetheless, the known radio polarization properties of the region seem to give some clue about the origin of the abrupt bend in the jet flow near B_N. According to Gardner and Whiteoak (1971), the degree of linear polarization at 5 GHz is very high in this region, attaining a maximum of $\sim$70% but generally remaining above 50% over a sizable area around B_N. This implies a highly ordered magnetic field which they found to be aligned in PA $\sim 144^{\circ}$ near the peak B_N. The field would thus be roughly orthogonal to the direction of the jet flow into the region of B_N. Note that the jet momentum and energy density has presumably greatly decreased by this stage owing to lateral expansion (Fig.7.1a; 7.1c) and therefore, it is quite plausible that the dynamics of the jet is hereafter determined by the (well ordered) magnetic field. As seen from Fig.7.1c, there is indeed a striking agreement between the radio continuum ridge and the magnetic field orientation, as given by Gardner and Whiteoak, for the region beyond the peak B_N. Indeed, an analogous process may be responsible for the radio spur seen extending eastward in the southern lobe of Cen A between declinations -44° and $-44^{\circ}.5$ (Fig.7.1c). The linear polarization observations of this region, also carried out by Gardner and Whiteoak (1971), again indicate a very high degree of polarization (generally between 30% to 50% at 5 GHz) and a highly ordered magnetic field oriented east-west, i.e., parallel to the radio spur observed in this part (Fig.7.1c).

CONCLUSIONS

A detailed comparison of the deep radio, optical and X-ray maps of the nearest double radio galaxy Centaurus A has provided evidence to show that both the jet and counter-jet in this source have been substantially stalled after impinging on optically visible shell segments located many kiloparsec away from the galactic nucleus. This circumstance clearly appears to be responsible for the formation of radio hotspots marked as A_N and B_S (see Fig.7.1c and Fig.7.2a). The clockwise extension of radio contours, as witnessed in both these and several other prominent radio peaks in this source (Fig.7.1 and Fig.7.2), as well as their inversion symmetric configuration with respect to the nucleus can be understood if one postulates a general clockwise rotation field for all the optically detected shell segments and circumgalactic medium asociated with Cen A. This scenario could be an alternative to the hypothesis of a sustained anti-clockwise precession of the central engine, as proposed by some authors (e.g., Haynes et al., 1983). Our proposition gains support from the observed spatial coincidence between the bright radio and optical features revealed by the recent deep observations of Cen A. Further, in view of such spatial coincidence, it appears likely that the radio peaks often develop where the relativistic plasma, either inside the jet or within the lobes, happens to encounter complexes of thermal gas and stars. Thus, it may not be essential to invoke repetitive outbursts of nuclear activity in order to understand the multiplicity of radio peaks on the opposite sides of the nucleus of this galaxy. A more comprehensive analysis of the situation would be possible by obtaining a high-contrast photograph of Cen A similar to that reproduced in Fig.7.1b, but covering the entire area all the way to the outermost radio peaks in the lobes of Cen A.

The deflection of the jet due to encounter with the shell segment 9 and the resultant formation of the north-eastern inner radio lobe (A_N), as proposed in our model, seems feasible for a gas density in the shell of $\geq 3.10^{-28}$ gm cm^{-3}. If, as in the case of this radio lobe, the shell responsible for the formation of any given radio lobe can be identified, the age of the lobe could be estimated by considering the dynamics of the interacting shell. A knowledge of the age, coupled with any observed break in the spectrum could afford a promising means of estimating the magnetic field strength inside radio lobes of active galaxies, without resorting to the assumption of minimum energy or minimum pressure condition.

CHAPTER VIII

CONSTRAINTS ON SOME PHYSICAL PARAMETERS OF CLASSICAL DOUBLE RADIO SOURCES

8.1 INTRODUCTION

Radio galaxies with their classical double radio morphology are best understood in terms of the continuous beam model (Blandford and Rees, 1974; Scheuer, 1974). In this model, basically there is a continuous supply of energy from the active nucleus of the parent galaxy to the outer regions, in the form of a pair of anti-parallel "jets" or "beams" of relativistic plasma and magnetic field. In the case of powerful radio galaxies, the beams are thought to be supersonic, which upon impinging on the external medium create shocks on either side of the 'contact discontinuity'. In the region after the reverse shock, the directed flow of the beam plasma gets disrupted and the velocities are significantly randomized. The ensuing substantial radiative losses in that region give rise to a radio "hotspot". Only a fraction of the kinetic power of the beam plasma is used up in producing relativistic plasma inside the hotspot and of that only a fraction is lost as radiation. While radiating away part of their energy inside the continuously advancing hotspot, the particles are subjected to the ram pressure of the external medium and, thus, stream in the direction of the nucleus, filling an extensive region called a "lobe" or "bridge". In this region the electrons with reduced energies (due to adiabatic expansion losses) radiate in diluted magnetic fields.

Intrinsic parameters derived from the observations of these sources are essential for arriving at an understanding of the relevant physical processes. In this chapter we obtain some of the intrinsic parameters using a representative sample of 10 bright, powerful ($L \sim 10^{44\pm1} ergs^{-1}$) hotspots (Saripalli and Gopal-Krishna, 1985). This approach, also employed by Perley et al. (1984),is based on the energetics and dynamics of the jet-hotspot interaction. Such a study is normally possible only for powerful double radio sources which possess hotspots near their extremities (Fanaroff and Riley, 1974).

To relate any of the observed parameters to the intrinsic parameters of a radio source like its beam power, it is essential to know the level of efficiency with which the bulk kinetic energy of the beam gets converted into radio power. For example, a powerful radio source could be formed with intrinsically weak beams provided the conversion efficiency is high and vice versa. Giant radio galaxies are examples where although they appear to be relatively weak in their radio output (Saripalli et al., 1986), their beams are, very likely intrinsically powerful (Gopal-Krishna, Wiita and Saripalli, 1988; also see Chapter VI). The determination of this efficiency factor is difficult, as one must include all possible loss mechanisms like adaibatic expansion losses, inverse Compton losses, losses incurrerd due to entrainment

(De Young, 1986), thermal plasma heating (Eilek, 1982) etc. Moreover, these are all model dependent (see Rawlings and Saunders, 1988). Even so, values of 1-30% have been estimated for the conversion efficiency in the literature (Dreher, 1984; Begelman, Blandford and Rees, 1984; Gopal-Krishna and Saripalli, 1984a; Gopal-Krishna, Wiita and Saripalli, 1988).

In this chapter we use the observed jet-hotspot properties of 10 powerful sources, possessing bright, compact hotspots, to calculate the efficiency of conversion of beam power into synchrotron radio power from the hotspot, making some simple assumptions, which are spelled out in the next section. Also, since the efficiency is always well below unity, the analysis yields rather stringent lower limits to the bulk velocity of the beam material (which cannot be measured directly).

From a variety of observational evidences, it is well established that the beams are relativistic on parsec scales (see, Bridle and Perley, 1984; Begelman, Blandford and Rees, 1984). However, on the kilo-parsec scales the situation is far from being clear (see review by Bridle, 1986). Support for relativistic velocities on kiloparsec scales comes from the observed one-sidedness of parsec and kilo-parsec jets occurring on the same side of the nucleus (Scheuer, 1987), and more recently, from the depolarization asymmetries in the lobes of classical double radio sources (Laing, 1988). However, the predominance of one-sided kilo-parsec jets in quasars (Bridle, 1986) is taken as evidence against relativistic jet velocities on kilo-parsec scales (see however, Kundt and Gopal-Krishna, 1981). Employing the above mentioned idea of jet-hotspot interaction, we obtain limits for the beam bulk velocities for sources in our sample of compact, powerful hotspots. The bulk streaming velocity of the relativistic electrons outflowing from the hotspot into the lobe is again poorly known. The distribution of the magnetic field in the hotspot might significantly govern the flow speeds of the electrons (Eilek, 1982). The method described in Section 8.1 provides limits to the outflow velocity of the plasma within individual hotspots (Saripalli and Gopal-Krishna, 1985).

The dependence of radio structure on the luminosity of radio galaxies is well known (Fanaroff and Riley, 1974). As shown by Jenkins and McEllin (1977), the fractional flux in the hotspots [defined as C = (Flux density from hotspot < 15 kpc in extent)/(total flux density-flux density excluding the central component)] increases with the total radio luminosity, L, of the source. In Section 8.2, we sketch a scenario based on the beam model, and on the simple assumptions namely, an equipartition of energy between the radiating particles and magnetic field and a spherical shape for the hotspots, to explain the C-L correlation. New inter-relationships between the source luminosity and hotspot properties are derived. It is found that hotspots powered by non-relativistic beams ($V_b \leq 0.1c$) can atmost attain luminosities of $\sim 10^{44}$erg s^{-1}, while those powered by relativistic beams can attain much higher luminosities. A distinct change in the morphology of the hotspots is found to occur for luminosities $\gtrsim 10^{46}$ erg s^{-1} (Gopal-Krishna and Saripalli, 1984a). The slab-like geometry inferred for such powerful hotspots resembles the reported sub-arcsecond resolution maps of hotspots in some powerful radio sources (Dreher, 1981; Begelman, Blandford and Rees, 1984).

8.1.1 Constraints on the jet/hotspot parameters

The Sample : Each of the selected 10 hotspots in our sample is radio luminous ($L \sim 10^{44 \pm 1}$ erg s^{-1}) and compact, having a radius $r_{hs} \leq 1$ kpc which is atleast 100 times smaller than the overall size of the associated radio source. The observed parameters of these representative, bright hotspots are listed in Table 8.1.1. Also listed are the flux density S_o at some frequency ν_o and the ratio of the hotspot flux to that of the radio lobe associated with it. A Hubble constant of $H_o = 75$ kms^{-1} Mpc^{-1} and $q_o = 0$ have been used in this section.

Assumptions : The hotspots are assumed to be spherical and filled uniformly with relativistic electrons and magnetic field, radiating under the condition of minimum energy density (Burbidge, 1959). The radio spectrum of the hotspot is assumed to be straight between a turnover frequency ν_t, due to synchrotron self-absorption, and an upper limiting frequency $\nu_u = 10$ GHz (Scheuer, 1982).

Table 8.1.1 The observed parameters of the 10 hot spots

Source (hot spot)	z	Overall size of the radio source		r_{hs}		S_0(hot spot) at ν_0		$\left(\frac{S_0}{S_{lobe}}\right)_{\nu_0}$	Ref.
		(″)	(kpc)	(″)	(kpc)	(Jy)	(GHz)		
0312−034 (SW 2) (4C−03.11)	1.072	42	317	0.12	0.91	0.076	(4.87)	0.46	1
0610+260 (NW) (3C 154)	0.580	51	297	0.025	0.15	0.75	(0.327)	0.10	2–4
0835+580 (SW 1) (3C 205)	1.534	17	140	0.011	0.09	0.66	(1.666)	0.50	5, 1
0843+136 (SW) (4C 13.39)	1.875	2	17	$\lesssim$0.01	$\lesssim$0.08	0.18	(1.417)	–	6
1137+660 (SE) (3C 263)	0.652	44	272	$\lesssim$0.11	$\lesssim$0.68	0.516	(4.87)	0.74	1, 7
1206+439 (SW) (3C 268.4)	1.400	10	81	0.1	0.81	0.5	(1.417)	0.33	6, 8
1957+405 (SE) (Cygnus A)	0.056	124	127	0.6	0.62	10	(22.5)	0.36	9, 10
2325+293 (SE 2) (4C 29.68)	1.015	50	370	0.14	1.04	0.07	(4.87)	0.33	1
2338+042 (SE) (4C 04.81)	2.594	3	27	0.01	0.09	0.46	(1.417)	–	6, 11
2354+144 (SE) (4C 14.85)	1.810	11	93	0.015	0.13	0.05	(1.417)	0.07	6, 8

References: (1) Swarup et al. (1984); (2) G. Swarup (private communication); (3) Kapahi et al. (1974); (4) S. Ananthakrishnan (private communication 1983); (5) Lonsdale and Barthel (1984); (6) Barthel (1983); (7) Owen et al. (1978); (8) Hintzen et al. (1984); (9) Dreher (1981); (10) Dreher (1979); (11) Barthel and Lonsdale (1983)

8.1.2 The Estimated Jet/Hotspot Parameters

The value of ν_t is computed using the following expression (Kellermann and Pauliny-Toth, 1981) and is adjusted iteratively to become consistent with the minimum energy condition

$$\nu_t(\mathrm{MHz}) = 33\ B^{1/5}\ \theta^{-4/5}\ S_{peak}^{2/5}\ (1+z)^{1/5} \qquad \ldots(8.1)$$

Here B is the magnetic field (Gauss), θ is angular size (arcsec), z is redishift and S_{peak} is the peak flux density (Jy) extrapolated from the observed flux density S_o at a frequency ν_o where the hot spot is transparent, using a spectral index .

$$S_{peak} = S_o(\nu_o/\nu_t)^{\alpha}$$

Now, assuming the hot spot to be in a steady state, maintaining a pressure balance with the directed pressure of the jet fluid, one gets in the frame of the hot spot:

$$\rho_j\ V_j^2\ \gamma_j^2 = u_{hs}/3 \qquad \ldots(8.2)$$

where ρ_j and V_j are the density and bulk velocity of the jet fluid, respectively and γ_j is the bulk Lorentz factor $= [1-(V_j/c)^2]^{-1/2}$. Now, if the jet kinetic power, L_j, gets converted into radiation inside the hot spot with a net efficiency ϵ , then:

$$L_j = L_{hs}/\varepsilon = \pi r_j^2\ \rho_j\ c^2 V_j\ \gamma_j\ (\gamma_j - 1) \qquad \ldots(8.3)$$

Eliminating ρ_j from Eq.(8.2) and Eq.(8.3):

$$\varepsilon = 3.18.10^{-11}\ .\ \frac{L_{hs}}{u_{hs}\ r_j^2}\ \left(\frac{\gamma_j + 1}{\gamma_j - 1}\right)^{1/2} \qquad \ldots(8.4)$$

A lower limit to ϵ is obtained by considering the maximum possible values for γ_j and r_j (i.e., $\gamma_j = \infty$ and $r_j = r_{hs}$); these values of ϵ_{min} are given in Table 8.1.2. We adopt 0.3 as the maximum possible value of ϵ, which is well below unity, since a good fraction of the energy supplied to the hot spots does not get radiated away within them but flows out, giving rise to diffuse radio lobes (Table 8.1.1; also see Gopal-Krishna and Saripalli, 1984a). Thus, for the maximum possible values of ϵ and r_j (i.e., $\epsilon = \epsilon_{max} = 0.3$ and $r_j = r_{hs}$), Eq.(8.4) yields a lower limit to V_j (Table 8.1.2). The V_j^{min}, in turn, yields via Eq.(8.2) the maximum rest-mass density of the jet material. The computed values of ρ_j^{max} are given in Table 8.1.2, together with those of the maximum rest-mass flux flowing through the jet: $\dot{M}_j^{max}$, where $\dot{M}_j = \pi r_j^2 \rho_j V_j \gamma_j = \pi r_j^2 \rho_j (u_{hs}/3\rho_j)^{1/2}$ and hence $\dot{M}_j^{max} = \dot{M}_j^{max} = \pi r_{hs}^2 (u_{hs} \rho_j^{max}/3)^{1/2}$ [see Eq.(8.2)].

The above estimates of the efficiency ϵ with which the jet fluid (synchrotron plasma) injected into the hotspot gets converted into radiation can be used to determine the bulk outflow speed, V_{out}, of the synchrotron plasma from the hotspots. If $\tau \sim r_{hs}/V_{out}$ is the average time spent by a volume element of the synchrotron plasma inside the hot spot of total volume V_{hs}, starting from the moment of its injection at the jet outlet (=shock front) presumably located near the centre of the hot spot, then

$$\epsilon = \tau(L_{hs}^{bol}/V_{hs})(U_{hs}/V_{hs}) \sim r_{hs} L_{hs}^{bol}/U_{hs} V_{out} \qquad \ldots(8.5)$$

Here U_{hs} is the energy in the hot spot. Now, from Eqs.(8.4) and (8.5):

$$V_{out} \sim 0.25c\,\{(\gamma_j - 1)/(\gamma_j + 1)\}^{1/2}\,\left(\frac{r_j}{r_{hs}}\right)^2 \qquad \ldots(8.6)$$

Evidently, the outflow speed of the relativistic plasma from a hot spot increases with the jet velocity and attains a maximum, $V_{out} \sim 0.25$ c for the maximum possible values of γ_j and r_j (i.e., $\gamma_j = \infty$ and $r_j = r_{hs}$). A lower limit to V_{out} for each hot spot, derived by setting $\epsilon = \epsilon_{max} = 0.3$ in Eq.(8.5), is given in Table 8.1.2. The range, thus estimated for V_{out}, defines a range for the average time τ which the synchrotron plasma is expected to spend within the hot spot. These limiting values of τ, in turn, yield the expected range for the frequency ν_b, above which synchrotron losses would steepen the spectrum ($\nu_b = 10^{24} V_{out}^2 B^{-3} r_{hs}^{-2}$). As seen from Table 8.1.2, the derived range for ν_b for all the hot spots encompasses the originally assumed value of ν_u = 10 GHz. Such a consistency check was found to limit the initial choice of ν_u to a maximum of the order of 100 GHz for all the 10 hot spots

Further, for each hot spot, we have given in Table 8.1.2, the estimated upper limit to the thermal gas density, ρ_{hs}^{max} (as well as the corresponding upper limit to the mass, M_{hs}^{max}). These are evaluated by considering that the outflow seed V_{out} of the relativistic electrons, estimated above, should not exceed the Alfven speed: $V_A = B_{hs}(4\pi\rho_{hs})^{-1/2}$. This gives $\rho_{hs}^{max} = (B_{hs}/V_{out}^{min})^2/4\pi$. The last column in Table 8.1.2

Table 8.1.2 The derived physical parameters of the hot spots and of the associated jets*

Name	ν_t	L_{hs}^{bol}	U_{hs}^{min}	u_{hs}^{min}	B_{hs}^{min}	ε_{min}	V_j^{min}	ϱ_j^{max}	$\dot{M}_j^{max}$	V_{out}^{min}	Range for ν_b	ϱ_{hs}^{max}	M_{hs}^{max}	γ_e^{min}
	MHz	erg s^{-1}	erg	erg cm^{-3}	Gauss			gm cm^{-3}	$M_\odot$ yr^{-1}		GHz	gm cm^{-3}	$M_\odot$	
0312 − 034 (SW 2)	28.7	4.2 10^{43}	6.2 10^{56}	7.1 10^{-9}	2.8 10^{-4}	0.025	0.163c	9.7 10^{-29}	0.187	0.021c	2.4–349	1.6 10^{-26}	7.4 10^{5}	230
	46.6	7.1 10^{43}	9.3 10^{56}	1.1 10^{-8}	3.4 10^{-4}	0.028	0.186c	1.1 10^{-28}	0.248	0.023c	1.7–191	1.8 10^{-26}	8.3 10^{5}	266
0610 + 260 (NW)	115.0	1.7 10^{43}	3.2 10^{55}	8.5 10^{-8}	9.6 10^{-4}	0.032	0.211c	6.8 10^{-28}	0.044	0.027c	3.7–320	1.1 10^{-25}	2.1 10^{4}	218
	125.2	1.1 10^{43}	2.8 10^{55}	7.4 10^{-8}	8.9 10^{-4}	0.024	0.162c	1.0 10^{-27}	0.050	0.020c	2.6–390	1.7 10^{-25}	3.3 10^{4}	236
0835 + 580 (SW1)	336.9	3.4 10^{44}	8.0 10^{55}	8.8 10^{-7}	3.1 10^{-3}	0.159	0.829c	1.5 10^{-28}	0.026	0.133c	7.0– 25	4.8 10^{-26}	2.2 10^{3}	262
	390.2	3.5 10^{44}	8.2 10^{55}	9.1 10^{-7}	3.1 10^{-3}	0.158	0.823c	1.6 10^{-28}	0.027	0.131c	6.5– 24	5.0 10^{-26}	2.3 10^{3}	282
0843 + 136 (SW)	226.6	1.5 10^{44}	4.9 10^{55}	6.4 10^{-7}	2.6 10^{-3}	0.111	0.651c	3.2 10^{-28}	0.028	0.093c	6.2– 45	7.1 10^{-26}	2.6 10^{3}	250
	268.3	1.6 10^{44}	5.1 10^{55}	6.7 10^{-7}	2.7 10^{-3}	0.110	0.647c	3.4 10^{-28}	0.029	0.092c	5.7– 42	7.6 10^{-26}	2.8 10^{3}	267
1137 + 660 (SE)	58.1	8.3 10^{43}	6.1 10^{56}	1.6 10^{-8}	4.2 10^{-4}	0.038	0.247c	9.2 10^{-29}	0.154	0.031c	2.8–179	1.6 10^{-26}	3.1 10^{5}	239
	88.1	1.3 10^{44}	8.4 10^{56}	2.2 10^{-8}	4.9 10^{-4}	0.042	0.274c	1.0 10^{-28}	0.188	0.035c	2.2–110	1.7 10^{-26}	3.3 10^{5}	272
1206 + 439 (SW)	52.4	2.4 10^{44}	1.4 10^{57}	2.2 10^{-8}	4.8 10^{-4}	0.059	0.378c	4.8 10^{-29}	0.185	0.049c	3.2– 82	8.6 10^{-27}	2.8 10^{5}	256
	71.1	2.9 10^{44}	1.6 10^{57}	2.6 10^{-8}	5.3 10^{-4}	0.058	0.373c	5.9 10^{-29}	0.223	0.048c	2.4– 63	1.0 10^{-26}	3.3 10^{5}	284
1957 + 405 (SE)	60.7	2.2 10^{43}	2.6 10^{56}	9.6 10^{-9}	3.2 10^{-4}	0.021	0.140c	1.8 10^{-28}	0.137	0.018c	2.4–490	3.0 10^{-26}	4.3 10^{5}	224
	106.5	4.7 10^{43}	4.3 10^{56}	1.6 10^{-8}	4.2 10^{-4}	0.027	0.179c	1.8 10^{-28}	0.176	0.023c	1.9–225	3.0 10^{-26}	4.3 10^{5}	259
2325 + 293 (SE 2)	24.5	3.4 10^{43}	6.7 10^{56}	5.1 10^{-9}	2.3 10^{-4}	0.021	0.141c	9.4 10^{-29}	0.204	0.018c	2.2–438	1.6 10^{-26}	1.1 10^{6}	232
	40.4	5.9 10^{43}	1.0 10^{57}	7.7 10^{-9}	2.9 10^{-4}	0.024	0.160c	1.1 10^{-28}	0.271	0.020c	1.5–234	1.8 10^{-26}	1.2 10^{6}	265
2338 + 042 (SE)	340.3	8.3 10^{44}	1.2 10^{56}	1.4 10^{-6}	3.9 10^{-3}	0.244	0.979c	2.3 10^{-29}	0.013	0.203c	8.2– 12	3.3 10^{-26}	1.5 10^{3}	280
	388.2	8.5 10^{44}	1.3 10^{56}	1.5 10^{-6}	4.0 10^{-3}	0.244	0.979c	2.3 10^{-29}	0.013	0.204c	7.9– 12	3.3 10^{-26}	1.5 10^{3}	295
2354 + 144 (SE)	103.2	4.4 10^{43}	4.4 10^{55}	1.7 10^{-7}	1.4 10^{-3}	0.053	0.341c	4.9 10^{-28}	0.040	0.044c	4.4–143	8.6 10^{-26}	1.1 10^{4}	228
	131.6	5.0 10^{43}	4.9 10^{55}	1.9 10^{-7}	1.4 10^{-3}	0.053	0.342c	5.5 10^{-28}	0.045	0.044c	3.7–120	9.6 10^{-26}	1.2 10^{4}	257

* The values given in the first and second row for each hot spot refer to $\alpha = -0.6$ and -0.9, respectively. (α is defined as: $S_\nu \sim \nu^\alpha$). These values of α essentially cover the range relevant for hot spots (e.g., Miley, 1980; Bedford et al., 1981)

gives for each hot spot the Lorentz factor γ_e^{min} down to which, at least, the energy spectrum of the relativistic electrons should continue to rise. In terms of the spectral turnover frequency ν_t (Table 8.1.2), it is expressed as:

$$\gamma_e^{min} \sim 0.5[\nu_t(1+z)/B_{hs}]^{1/2}$$

8.1.3 Discussion

The limits to the various jet parameters, as derived above, within the framework of the beam model, are conservative estimates since they refer to the maximum possible value of the jet radius (i.e., $r_j = r_{hs}$). As seen from Table 8.1.2, the hot spots in our sample must radiate away the jet kinetic power supplied to them at a minimum efficiency of 2-25%. Clearly, these lower limits to ϵ would have to be relaxed, should the hot spots depart from the assumed condition of minimum total energy (Eq.8.4). But, from the available evidence, this assumption appears to broadly apply for such extended radio structures (Scott and Readhead, 1977; Marshall and Clark, 1981; Scherier et al., 1982; Roland, 1982; (Chapter VII). Secondly, the adopted upper limit of $\epsilon_{max} = 0.3$ yields a range c/7-c for the <u>minimum</u> bulk velocities (V_j^{min}) for the beam fluid feeding the hot spots, as well as a range of 0.02c - 0.2c for the <u>minimum</u> bulk outflow velocities (V_{out}^{min}) of relativistic plasma from the hot spots. But, as in the case of ϵ, the derived lower limits to both V_j and V_{out} are dependent on the assumption of minimum energy for the hot spots. On the other hand, they would not be violated on account of the other assumption made in the previous section, that the spectra of the hotspots remains straight only up to 10 GHz. The same applies to the parameters ρ_j^{max}, $\dot{M}_j^{max}$, and ρ_{hs}^{max}, given in Table 8.1.2. It may also be noted from Eq.(8.6), that the outflow velocity V_{out} of relativistic plasma from the hot spots is expected to be higher for faster jets, attaining a maximum value of $\sim 0.25c$ for an ultra-relativistic jet. The upper limit does not depend on the assumption of minimum energy condition [Eq.(8.6)]. Another parameter which is fairly insensitive to this assumption is γ_e^{min} which represents the Lorentz factor below which the energy spectrum of relativistic electrons responsible for the radio output from the hot spot cuts off [from Eqs.(8.1) and (8.7); $\gamma_e^{min} \propto B^{-2/5}$]. From Table 8.1.2, it is seen that the values of γ_e^{min} for all the 10 hot spots lie in a rather narrow range: $\gamma_e^{min} = 250 \pm 50$. It is interesting that Faraday rotation measurements have indicated a similar lower limit to the Lorentz factors of relativistic electrons present inside compact radio sources coincident with active galactic nuclei (Wardle, 1977).

8.2. CONSTRAINTS ON THE LUMINOSITY ATTAINED BY HOTSPOTS

8.2.1 Some General Constraints on the Hotspots

The theory of synchrotron radiation tells us that the synchrotron luminosity L of a source increases not only with U, the total energy present in the form of relativistic electrons and magnetic field, but also with the pressure p due to them: $L \propto U.p^{3/4}$. Thus, for a given amount of beam power being discharged into the hot spot, the nonthermal radiation from the hot spot would be maximum when the pressure of the synchrotron plasma inside the hot spot is at the highest possible value. Here, one could place two general constraints on hot spots. Firstly, in order to ensure the flow of the beam plasma into the hotspot, the internal pressure of the hot spot p_{hs}, can at most be as high as the directed pressure of the beam plasma at the beam outlet, p_{bo} (we refer to this equilibrium configuration with $p_{bo} = p_{hs}$ as 'maximally radiating' hot spot). The second constraint is that the radius of the hot spot r_{hs}, cannot be smaller than the radius of the beam outlet, r_{bo}, around which the hot spot forms ($\eta = r_{hs}/r_{bo} \geq 1$). Thus, for estimating the maximum attainable radio luminosity, we express the first constraint pertaining to a maximally radiating hot spot, in steady state, as

$$[p_{bo} \sim L_{hs}/ \pi \varepsilon \beta c r_{bo}^2] = [p_{hs} \sim U_{hs}^{min}/4\pi r_{hs}^3] \qquad ...(8.7)$$

Here βc is the bulk velocity of the beam plasma whose kinetic power $L_b = L_{hs}/\epsilon$ gets converted into radio luminosity L_{hs} of the hot spot with the net conversion efficiency ϵ . U_{hs}^{min} is the total energy inside the hot spot in the form of magnetic field and relativistic electrons, computed for the usual equipartition condition defined by Burbidge (1959) (we shall ignore other possible forms of energy). If, now, one makes a reasonable assumption that the power radiated from the hot spot is mainly concentrated within the frequency range 100 MHz to 10^4 MHz (the results are not very sensitive to an order-of-magnitude uncertainty in these figures) with a spectral index $\alpha = +0.75$ (defined as : $S_\nu \propto \nu^{-\alpha}$) one obtains from the synchrotron theory (Moffet, 1968).

$$U_{hs}^{min} \simeq 2.6.10^4 \left(\frac{L_{hs}}{erg/s}\right)^{4/7} \left(\frac{r_{hs}}{cm}\right)^{9/7} erg. \qquad ...(8.8)$$

Combining Eq.8.7 and Eq.8.8 gives:

$$r_{hs}/r_{bo} = \eta = 1.4.10^7 (\beta\varepsilon)^{1/2} L_{hs}^{-3/14} r_{hs}^{1/7} . \qquad ...(8.9)$$

For r_{hs} on the right side, we substitute a single typical value of 1 kpc (Readhead and Hewish, 1976; Kerr et al., 1981; since the exponent is only 1/7, even an abnormally large deviation from this typical value would alter η very marginally). Eq.(8.9) thus reduces to:

$$L_{hs} \sim 5.10^{47} \eta^{-14/3} (\beta\varepsilon)^{7/3} \text{ erg s}^{-1} \qquad ...(8.10)$$

8.2.2. Efficiency and Bulk Velocity of a Beam and the Radio Luminosity

Among the 3 variables on the right side in Eq.8.10, both β and ϵ must clearly be <1 and η must be $\geq$ 1, as discussed earlier. In reality, the efficiency ϵ is expected to be well below 100%. This reasonable expectation is also consistent with the observation that even in highly luminous double sources a small amount of radio emission does arise from lobes surrounding the hot spots (e.g., Swarup et al., 1984;

Barthel, 1983). Most probably such lobes are formed due to relativistic electrons escaping out of the hot spots and therefore radiating less efficiently owing to weaker magnetic field, expansion losses and reduced energy density (e.g., Scott, 1977). Thus, even though the contribution of the lobes to the total radio output is marginal in case of highly luminous sources, as emphasized by Jenkins and McEllin (1977), their total energy content is large, indicating a high rate of energy leakage from the hot spots. Based on such considerations we adopt a reasonable upper limit of 0.3 to the value of efficiency with which the power delivered at the hot spot gets radiated away within the hot spots itself. Thus, together with the constraints $\eta \geq 1$ and $\epsilon \leq \epsilon_{max} = 0.3$, Eq.8.10 implies a maximum possible value of $L_{hs} \sim 10^{44}$ erg s^{-1} which can be attained for hot spots powered by non-relativistic beams having bulk velocities upto 0.1c. Also, it is seen that for relativistic beams with $\beta \sim 1$, L_{hs} of upto $\sim 3.10^{46}$ erg s^{-1} is attainable. In practice this limit would apply to the integrated radio luminosity of double sources, since it is known that in such highly luminous sources little emission arises from regions outside the hot spots (see Jenkins and McEllin, 1977; Swarup et al., 1984). In Section 8.2.3 we will discuss the possibility that the luminosity limit derived for relativistic beams may be surpassed because of a possible breakdown of our simplifying assumption of spherical geometry for the hot spots at such high luminosities. But this assumption seems justified for hot spots of moderate luminosities attainable with non-relativistic beams, which can emit upto $L_{max} \sim 10^{44}$ erg S^{-1} for the case $\beta = 0.1$ and $\epsilon = \epsilon_{max} = 0.3$, as discussed above. If, for the moment, the assumption of spherical geometry is retained for hot spots of all luminosities, then the following argument shows that the luminosity limits given above for non-relativistic and relativistic beams would hold even if the beam power is much higher than what is really necessary to produce hot spots of such luminositis; i.e., for $L_b \gg L_{max}(\epsilon, \beta)/\epsilon$. To illustrate this, let us rewrite Eq.(8.10) in terms of beam power L_b:

$$L_{hs}/\epsilon = L_b \simeq 5.10^{47}\, \eta^{-14/3}\, \beta^{7/3}\, \epsilon^{4/3} \text{ erg s}^{-1} \qquad \ldots(8.11)$$

Recalling that this expression characterizes a steady-state with a balance between P_{hs} and P_{bo} (via Eq.8.7), it is seen that for given ϵ and β there is a critical beam power $L_b^* \sim 5.10^{47} \beta^{7/3} \epsilon^{3/4}$ such that for a more powerful beam Eq.8.11 cannot be satisfied for physically meaningful values of η (i.e., for $\eta \geq 1$). For such an excessively powerful beam, therefore, the formation of the hot spot would involve an <u>inequilibrium</u> sitution. This is because the physical constraint $\eta \geq 1$ would force the hot spot to expand continuously from the (fictitious) equilibrium situation, with $P_{hs} \sim P_{bo}$ which for beams having $L_b > L_b^*$ is only possible when $\eta \leq 1$ (Eq.8.11). The resultant expansion by a factor η^{-1} <u>or more</u> implies rapid adiabatic loss, lowering the synchrotron luminosity by a factor $\geq \eta^4$ below the (fictitious) equilibrium situation (see Eq.8.8). Thus, for an excessively powerful beam with $L_b > L_b^* \sim 5.10^{47}\ \beta^{7/3} \epsilon^{4/3}$ (see above), L_{hs} would be $\lesssim \epsilon L_b \eta^4 \simeq 8.10^{40}\ \beta^2\ \epsilon^{15/7}$ $L_b^{1/7}$. This gives, even for a highly efficient ($\epsilon = \epsilon_{max}$ = 0.3), and excessively powerful beam (L_b say 10^{48}ergs^{-1}) L_{hs} of $\sim 4.10^{44}$ erg s^{-1} if $\beta = 0.1$ and $L_{hs} \sim 4.10^{46}$ erg s^{-1} if $\beta \sim 1$. These values are broadly consistent with the limits deduced above for non-relativistic and relativistic beams, respectively (see Gopal-Krishna and Saripalli, 1984a.)

8.2.3. Dependence of Hot Spot Size on Luminosity

To illustrate the inter-relationship between the luminosity of a hot spot, its size and beam efficiency, as expected in our model, we have given in Table 8.2.1 the values of η computed for a range of L_{hs} and ϵ using Eq.8.10. The values correspond to an ultra-relativistic beam velocity (β = 0.99) except for those given inside brackets which refer to a non-relativisitic beam with β = 0.1. For each value of L_{hs} we have also tabulated, in the last column, the minimum value of beam efficiency ϵ_{min} that would be required to attain the luminosity L_{hs} given in the first column. These limiting values correspond to the case when β = 0.99 and the hot spot not only radiates maximally (P_{hs} = P_{bo}) but also has the smallest possible size (r_{hs} = r_{bo}, i.e., η = 1), thereby maximising the radiative output (Eq.8.10). It is evident from Table 8.2.1 that for a given beam efficiency ϵ , the factor η (=r_{hs}/r_{bo}) increases towards smaller L_{hs}, i.e., for lower beam power ($L_b = L_{hs}/\epsilon$) which

Table 8.2.1. *The computed values of η ($=r_{hs}/r_{bo}$) as a function of beam efficiency (ϵ) and hot spot luminosity ($L_{hs} = \epsilon L_b$). The values of η given outside and inside brackets refer to $\beta = 0.99$ and $\beta = 0.1$, respectively. The minimum required efficiency, ϵ_{min}, is computed for the case $\beta = 0.99$ and $\eta = 1$ (eq. 8.10 Sect 8.2.3).*

L_{hs} (erg/s)	ϵ =100%	ϵ =30%	ϵ =10%	ϵ =3%	ϵ_{min} (%)
10^{41}	26.7 (8.5)	14.6 (4.7)	8.5 (2.7)	4.6 (1.5)	0.1 (1.4)
10^{42}	16.3 (5.2)	8.9 (2.8)	5.2 (1.6)	2.8 (0.9)	0.4 (3.7)
10^{43}	10.0 (3.2)	5.5 (1.7)	3.2 (1.0)	1.7 (0.5)	1.0 (10.1)
10^{44}	6.1 (1.9)	3.3 (1.1)	1.9 (0.6)	1.1	2.7 (27.0)
10^{45}	3.7 (1.2)	2.0 (0.6)	1.2	0.6	7.2 (72.4)
10^{46}	2.3 (0.7)	1.2	0.7		19.4 (194)!
10^{47}	1.4	0.8			52.1
10^{48}	0.8				140 !

would produce weaker radio sources. Since outlets of beams associated with lower luminosity sources are neither known nor expected to be systematically smaller (Bridle, 1986), the above mentioned dependence of η would predict that the hot spots associated with lower luminosity sources should be larger in size and thus appear more diffuse. Quantitatively, if one were to define hot spot as a region falling within a circular aperture of a fixed linear radius of, say, a few kpc (e.g., Jenkins and McEllin, 1977), such an aperture would be increasingly 'resolving' the hot spots associated with sources of decreasing luminosity because of their being systematiclly larger. This could explain the known positive correlation between the radio luminosity of a double source and the fraction of the total extended radio emission that arises from its hot spots. As mentioned above, such a correlation was first noted by Jenkins and McEllin (1977) for 3CR sources and more recently supported by Swarup et al. (1984) from VLA observations of a sample of steep spectrum quasars.

8.2.4. The Beam Power and Morphology of Hot Spots

From the discussion following Eq.8.11, L_{hs} appears to saturate for beam powers above a critical value L_b which could be as high as $(L_b)_{max} \approx 10^{46}$ erg s^{-1}, corresponding to the maximum adoptable values of $\beta(=1)$ and $\epsilon(=0.3)$. It was pointed out that higher beam power would induce onset of expansion of the hot spot from the equilibrium configuration, leading to a diminishing of volume emissivity as well as magnetic field strength, which had both been increasing steadily with beam power until the point of inequilibrium was reached owing to the constraint $\eta \geq 1$. But, of course, this constraint could be meaningfully imposed only provided our assumption of spherical geometry for the hot spots remained valid at least until they reached the point of inequilibrium. If prior to this point, the hot spots were to somehow develop a slab-like geometry, then by arbitrarily compressing the slab along the beam direction, P_{hs} could be maintained equal to P_{bo} (to ensure equilibrium) while the surface of the slab in contact with the beam outlet would continue to keep the latter fully covered. Thus, once a slab-like geometry has developed, the volume of the hot spot could arbitrarily reduce to maintain pressure equilibrium with a beam of arbitrarily high power and, accordingly, its luminosity could increase unconstrained. The crucial transformation from the spherical to slab-like geometry while the luminosity and the magnetic field of the hot spot are still rising with increasing beam power (i.e., before the point of inequilibrium is reached) could conceivably occur if the megnetic field in the hot spot has increased to a sufficiently high value. The relativistic electrons injected into the hot spot after randomization of their momenta at the beam outlet (=shock front) would then have synchrotron lifetimes, τ_{syn}, shorter than the light travel time, τ_{bo}, across the beam outlet, leading to the development of a slab-shaped hot spot. Such a condition would simply be satisfied by electrons having Lorentz factors $\gamma_{crit} > 1.5.10^{19}/r_{bo}\, B^2_{hs}$

where B_{hs} is the equipartition magnetic field equal to $[3 U_{hs}/\varkappa_{hs}]^{0.5}$. Eq.8.8 thus leads to:

$$\gamma_{crit} > 2.10^{14} \eta L_{hs}^{-4/7} r_{hs}^{5/7} \quad ...(8.12)$$

We substitute for r_{hs} a typical value of 1 kpc (see Section 8.2.1) and for L_{hs} the limiting luminosity of $\sim 10^{44}$ erg s^{-1} attainable for a hot spot powered by a non-relativistic beam ($\beta \leq 0.1$) before its equilibrium breaks down and the expansion of the hotspot begins. Since $\eta \geq 1$, Eq.8.12 thus gives $\gamma_{crit} > 3.10^{4}$. Thus, the condition for the formation of a slab-shaped hot spot would not be satisfied by all but the most energetic electrons. But they only form an energetically insignificant tail of the steeply falling electron energy distribution which probably peaks at $\gamma \approx 10^{2}$, as inferred for the hot spots in Cygnus A from the estimated magnetic field of $\sim 3.10^{-4}$ G and synchrotron self-absorption frequencies of $\sim$ 70 MHz (see Hargrave and Ryle, 1974; Simon, 1977; Saripalli and Gopal-Krishna, 1985). In contrast, as discussed in Section 8.2.2, for a relativistic beam velocity the point of inequilibrium would only be reached at $L_{hs} \sim 3.10^{46}$ erg s^{-1} and this means that γ_{crit} could decline almost to $\sim 10^{3}$ (Eq.8.12). Since electrons with $\gamma > 10^{3}$ probably form an energetically significant part of the entire population of relativistic electrons, the hot spot could conceivably transform into a slab shape before its size has reduced to that of the beam outlet, whereby the inequilibrium is expected to set in for a spherical hot spot.

Henceforth, with increasing beam power and L_{hs}, the constraint $\eta > 1$ would no longer be meaningfully imposed for obtaining an upper limit to L_{hs}, as discussed earlier.

8.3. CONCLUSION

Within the framework of the beam model we have deduced some basic physical parameters of the jets and hotspots associated with classical double radio sources, following a simple approach which is based on the assumptions that the hot spots radiate under the usual equipartition conditions and that they are roughly spherical in shape. For a sample of 10 bright hotspots and for the jets presumed to be feeding them, we have estimated the densities, bulk velocities, mass-flow rates and efficiencies of the jets. It is found that the bulk outflow velocity of the relativistic electrons present inside the hotspot, increases with the jet velocity and attains a maximum value of 0.25c (Saripalli and Gopal-Krishna, 1985).

A rather natural explanation is found for the known tendency of more prominent and compact hot spots to be associated with sources of higher luminosties. It is also argued that the maximum expected luminosities of hot spots are $\sim 10^{44}$ and $\sim 3.10^{46}$ erg s^{-1}, respectively, for beam velocities of $< 0.1c$ and $\sim c$. However, the latter limit could be surpassed due to a possible breakdown of the assumption of spherical shape for the hot spots at such high luminosities where their morphology could undergo a qualitative change and become slab-like (Gopal Krishna and Saripalli, 1984a).

REFERENCES

Adams, M.T., Jensen, E.B., Stocke, J.T. : 1980, Astron. J. **85**, 1010.

Alexander, P., Leahy, J.P. : 1987, Monthly Notices Roy. Astron. Soc. **225**, 1.

Andernach, H., Wielebinski, R. : 1982, Extragalactic Radio Sources, IAU Symp. **97**, p.13, eds Heeschen, D.S. and Wade, C.N.

Athanassoula, E., Bosma, A. : 1985, Annual Rev. Astron. Astrophys. **23**, 147.

Auriemma, KC., et al. : 1977, Astron. Astrophys. **57**, 41.

Baade, W., Minkowski, R. : 1954, Astrophys. J. 119, 215.

Baars, J.W.M., Genzel, R., Pauliny-Toth, I.I.K., Witzel, A. : 1977, Astron. Astrophys. **61**, 99.

Baldwin, J.E. : 1982, Extragalactic Radio Sources, IAU Symp. **97**, p 21, eds Heeschen, D.S. and Wade, C.N.

Baldwin, J.E., et al. : 1985, Monthly Notices Roy. Astron. Soc. **217**, 77.

Banhatti, D.G. : 1987, Monthly Notices Roy. Astron. Soc. **225**, 487.

Barcons, X. : 1987, Astrophys. J. **313**, 517.

Barcons, X., Fabian, A.C. : 1988, Monthly Notices Roy. Astron. Soc. **230**, 189.

Barthel, P.D. : 1983, Astron. Astrophys. **126**, 16.

Barthel, P.D., Lonsdale, C.J. : 1983, Monthly Notices Roy. Astron. Soc. **205**, 395.

Barthel, P.D., Schilizzi, R.T., Miley, G.K., Jagers, W.J., Strom, R.G. : 1985, Astron. Astrophys. **148**, 243.

Baum, S.A., Heckman, T., Bridle, A., van Breugel, W., Miley, G. : 1988, Astrophys.J. (in press).

Bedford, N.H. : 1981, Monthly Notices Roy. Astron. Soc. **195**, 245.

Begelman, M.C., Blandford, R.D., Rees, M.J. : 1984, Rev. Mod. Phys. **56**, 245.

Bicknell, G.V. : 1985, Proc. Astron. Soc. Aust. **6**, 130.

Biermann, P., Kronberg, P.P., Madore, B.F. : 1982, Astrophys. J. **256**, L37.

Blanco, V.M., Graham, J.A., Lasker, B.M., Osmer, P.S. : 1975, Astrophys. J. **198**, L63.

Blandford, R.D., Rees, M.J. : 1974, Monthly Notices Roy. Astron. Soc. **169**, 375.

Boldt, E. : 1987, Phys. Report : **146**, 215.

Bolton, J.G., Stanley, G.J., Slee, O.B. : 1949, Nature, **164**, 101.

Bolton, J.G., Gardner, F.F., Mackey, M.B. : Aust. J. Phys. **17**, 340.

Bosma, A., Smith, R.M., Wellington, K.J. : 1985, Monthly Notices Roy. Astron. Soc. **212**, 301.

Bridle, A.H. : 1984, Astron. J. **89**, 979.

Bridle, A.H. : Can. J. Phys. **64**, 353.

Bridle, A.. : 1987, in Proc. of Georgia State University Conference on 'Active Galactic Nuclei' eds. Miller, R. and Wiita, P.J.

Bridle, A.H., Davis, M.M., Fomalont, E.B., Lequeux, J. : 1972, Astron. J. **77**, 405.

Bridle, A.H., et al. : 1976, Nature **262**, 179.

Bridle, A.H., Fomalont, E.B., : 1979, Astron. J. **84**, 1679.

Bridle, A.H., et al. : 1979, Astrophys. J. **228**, L9.

Bridle, A.H., Fomalont, E.B., Cornwell, T.J. : 1981, Astron. J. **86**, 1294.

Bridle, A.H., Perley, R.A. : 1984, Annual Rev. Astron. Astrophys. **22**, 319.

Brodie, J., Konigl, A., Bowyer, S. : 1983, Astrophys. J. **273**, 154.

Brosch, N., Krumm, N. : 1984, Astron. Astrophys. **132**, 80.

Burbidge, G.R. : 1959, Astrophys. J. **129**, 849.

Burbidge, G.R., Crowne, A.H. : 1979, Astrophys. J. Suppl. 40, 583.

Burch, S.F. : 1979, Monthly Notices Roy. Astron. Soc. **186**, 293.

Burns, J.O., Basart, J.P., De Young, D.S., Ghiglia, D.C. : 1984, Astrophys. J. **283**, 515.

Burns, J.O., Feigalson, E.D., Schreier, E.J. : 1983, Astrophys. J. **273**, 128.

Burns, J.O., Owen, FN., Rudnick, L. : 1979, Astron. J. **84**, 1683.

Burns, J.O., et al. : 1987, Astron. J. **94**, 587.

Canizares, C.R., Fabbiano, G., Trinchieri, G. : 1987, Astrophys. J. **312**, 503.

Carter, D., Allen, D.A., Malin, D.F. : 1982, Nature 295, 126.

Christiansen, W.N., et al., : 1977, Monthly Notices Roy. Astron. Soc. **181**, 183.

Cooper, B.F.C., Price, R.M., Cole, D.J. : 1965, Aust. J. Phys. **18**, 589.

Cordey, R.A. : 1987, Monthly Notices Roy. Astron. Soc. **227**, 695.

Cowsik, R., Kobetich, E.J. : 1972, Astrophys. J. **177**, 585.
Danziger, I.J., Goss, W.M. : 1983, Monthly Notices Roy. Astron. Soc. **202**, 703.
Danziger, I.J., Goss, W.M., Frater, R.H. : 1978, Monthly Notics Roy. Astron. Soc. **184**, 341.
Demouline, M. : 1970, Astrophys. J. **160**, L79.
De Ruiter, H.R., Parma, P., Fanti, C., Fanti, R. : 1986, Astron. Astrophys. Suppl. **65**, 111.
De Young, D.S. : 1981, Nature **293**, 43.
De Young, D.S. : 1986, Astrophys. J. **307**, 62.
De Young, D.S., Axford, I. : 1967, Nature **216**, 129.
Dreher, J.W. : 1979, Astrophys. J. **230**, 687.
Dreher, J.W. : 1981, Astron. J. **86**, 833.
Dreher, J.W. : 1983, in Physics of Energy Transport in Extragalactic Radio Sources, p. 109, eds. Bridle, A.H., Eilek, J.A.
Dressel, L.L. : 1981, Astrophys. J. **245**, 25
Duffey-Smith, P. and Purvis, A. : 1982, in Extragalactic Radio Sources, IAU Symp. **97**, p 59, eds. Heeschen, D.S., Wade, C.N.
Dufour, R.J., van der Bergh, S. : 1978, Astrophys. J. **226**, L73
Dufour, R.J., et. al., 1979, Astron. J. **84**, 284.
Dupraz, C., Combes, F. : 1986, Astron. Astrophys. **166**, 53.
Eales, S.A. : 1985, Monthly Notices Roy. Astron. Soc. **217**, 179.
Eilek, J.A. : 1982, Astrophys. J. **254**, 472.
Ekers, R.D. : 1982, in Extragalactic Radio Sources, IAU Symp. **97**,p 465, eds Heeschen, D.S., Wade, C.N.
Ekers, R.D., Fanti, R., Lari, C., Parma, P. : 1978, Nature **276**, 768.
Ekers, R.D., Fanti, R., Lari, C., Parma, P. : 1981, Astron. Astrophys. **101**, 194.
Ekers, R.D., Simkin, S.M. : 1983, Astrophys. J. **265**, 85.
Ellis, R. : 1982, in Origin and Evolution of Galaxies, p 255, eds. Jones, B.J.T., Jones, J.E.
Fabbiano, G., Miller, L., Trinchieri, G., Longair, M., Elvis, M. : 1984, Astrophys. J. **277**, 115.
Fabian, A.C., Nulen, P.E.J., Stewart, G.C. : 1980, Nature **287**, 613.
Fanaroff, B.L., Riley, J.M. : 1974, Monthly Notices Roy. Astron. Soc. **167**, 31 p.
Fanti, R., Gioia, I., Lari, C., Ulrich, M.H. : 1978, Astron. Astrophys. Suppl. **34**, 341.
Fanti, C., et. al. : 1982, Astron. Astrophys. **105**, 200.
Fanti, C., Fanti, R., De Ruiter, H.R., Parma, P. : 1986, Astron. Astrophys. Suppl. **65**, 145.
Fanti, C., Fanti, R., De Ruiter, H.R., Parma, P. : 1987, Astron. Astrophys. Suppl. **69**, 57.
Faulkner, M. : 1986, Ph.D. Thesis, University of Cambridge.
Feigelson, E.D., Berg, C.J. : 1983, Astrophys. J. **269**, 400.
Feigelson, E.D., et. al. : 1981, Astrophys. J. **251**, 31.
Feretti, L., Giovannini, L., Gregorini, L., Parma, P., Zamorani, G. : 1984, Astron. Astrophys. **139**, 55.
Field, G., Perrenod, S. : 1977, Astrophys. J. **215**, 717.
Fokker, A.D. : 1986, Astron. Astrophys. **156**, 315.
Fomalont, E.B., Miley, G.K., Bridle, A.H. 1979, Astron. Astrophys. **76**, 106.
Forman, W., Jones, C., Tucker, W. : 1985, Astrophys. J. 293, 102.
Fort, B.P.,et. al. : 1986, Astrophys. J. **306**, 110.
Frogel, J.A., et. al. : 1987, Astrophys. J. **315**, L129.
Gardner, F.F., Whiteoak, J.B. : 1971, Aust. J. Phys. **24**,
Gavazzi, G., Perola, G.C. : 1978, Astron. Astrophys. **66**, 407.
Giacconi, R., Zamorani, G. : 1987, Astrophys. J. **313**, 20.
Giovannini, G., Feretti, L., Gregorini, L., Parma, P. : 1988, Astron. Astrophys. **199**, 73.
Gopal-Krishna, Chitre, S.M. : 1983, Nature **303**, 217.
Gopal-Krishna, Saripalli, L. : 1984a, Astron. Astrophys. **139**, L19.
Gopal-Krishna, Saripalli, L. : 1984b, Astron. Astrophys. **141**, 61.
Gopal-Krishna, Saripalli, L. : 1985, Astron. Astrophys. **149**, 205.
Gopal-Krishna, Saripalli, L., Saikia, D.J., Sramek, R.A. : 1986, in Quasars, IAU Symp **119**, p 193. eds Swarup, G., Kapahi, V.K.
Gopal-Krishna,Wiita, P.J. : 1988, Nature **333**, 49.

Gopal-Krishna, Wiita, P.J. : 1987, Monthly Notices Roy. Astron. Soc. **226**, 531.
Gopal-Krishna, Wiita, P.J., Saripalli, L. : 1988, Monthly Notices Roy. Astron. Soc. (in Press).
Goss, W.M., McAdam, W.B., ellington, K.J., Ekers, R.D. : 1987, Monthly Notices Roy. Astron. Soc. **226**, 979.
Graham, J.A. : 1979, Astrophys. J. **232**, 60.
Graham, J.A. : 1983, Astrophys. J. **269**, 440.
Graham, J.A., Price, R.M. : 1981, Astrophys. J. **247**, 813.
Graham, D.A., Weiler, K.W., Wielebinski, R. : 1981, Astron. Astrophys. **97**, 388.
Groth, E.J., Peebles, P.J.E. : 1977, Astrophys. J. **217**, 385.
Guilbert, P.W., Fabian, A.C. : 1986. Monthly Notices Roy. Astron. Soc. **220**, 439.
Guindon, B. : 1979, Monthly Notices Roy. Astron. Soc. **186**, 117.
Guthrie, B.N.G. : 1981, Monthly Notices Roy. Astron. Soc. **194**, 261.
Hargrave, P.J., McEllin, M. : 1975, Monthly Notices Roy. Astron. Soc. **173**, 37.
Hargrave, P.J., Ryle, M. : 1974, Monthly Notices Roy. Astron. Soc. **166**, 305.
Harris, A. : 1972, Monthly Notices Roy. Astron. Soc. **158**, 1.
Harris, A. : 1973, Monthly Notices Roy. Astron. Soc. **163**, 19p.
Haslam, C.G.T. : 1974, Astron. Astrophys. Suppl. 15, 333.
Haynes, R.F., Cannon, R.D., Ekers, R.D. : 1983, Proc. Astron. Soc. Aust. **5**,241.
Heckman, T.M., Carty, T.J., Bothun, G.D. : 1985, Astrophys. J. **288**, 122.
Henriksen, R.N., Vallee, J.P., Bridle, A.H. : 1981, Astrophys. J. **249**, 40.
Hesser, J.E., Harris, H.C., van den Bergh, S., Harris, G.L.H. : 1984, Astrophys. J. **276**, 491.
Hine, R.G. : 1979, Monthly Notices Roy. Astron. Soc. **189**, 527.
Hine, R.G., Longair, M.S. : 1979, Monthly Notices Roy. Astron. Soc. **188**, 111.
Hintzen, P., Ulvestad, J., Owen, F. : 1984, Astron. J. **88**, 709.
Hodges, M.W., Mutel, R.L. : 1986, in Superluminal Radio Sources, p 168, eds Zensus, J.A., Pearson, T.J.
Hogbom, J.A. : 1979, Astron. Astrophys. Suppl. **36**, 173.
Huang, S., Stewart, P. : 1985, Astron. Astrophys. **153**, 189.
Hummel, E., Kotanyi, C.G., Ekers, R.D. : 1983, Astron. Astrophys. **127**, 205.
Hutchings, J.B. : 1987, Astrophys. J. **320**, 122.
Hutchings, J.B., rampton, D., Campbell, B. : 1984, Astrophys. J. **280**, p41.
Jagers, W.J. : 1986, Ph.D. Thesis, University of Leiden.
Jagers, W.J., van Breugel, W.J.M., Miley, G.K., Schilizzi, R.T., Conway, R.G. : 1982, Astron. Astrophys. **105**, 278.
Jenkins, C.J., McElli, M. : 1977, Monthly Notices Roy. Astron. Soc. **180**, 219.
Jenkins, C.J., Pooley, G.G., Riley, J.M. : 1977, Mem. Roy. Astron. Soc. **84**, 61.
Johnson, H.M. : 1963, Publ. Natn. Radio Astron. Obs. **1**, 251.
Jones, D.L. : 1986, Astrophys. J. **309**, L5.
Jones, D.L., et al. : 1986, Astrophys. J. **305**, 684.
Kapahi, V.K. : 1978, Astron. Astrophys. **67**, 157.
Kapahi, V.K. : 1985, Monthly Notices Roy. Astron. Soc. **214**, 19p.
Kapahi, V.K. : 1986, Highlights of Astr. **7**, 371.
Kapahi, V.K., Gopal-Krishna, Joshi, M.N. : 1974, Monthly Notices Roy. Astron. Soc. **167**, 299.
Kellermann, K.I., Pauliney-Toth, I.I.K. : 1981, Annual Rev. Astron.Astrophys. **19**, 373.
Kellermann, K.I., Pauliny-Toth, I.I.K., Williams, P.J.S. : 1969, Astrophys. J. **157**, 1.
Kerr, A.J., Birch, P.A., Conway, R.G., Davis, R.J., Stannard, D. : 1981, Monthly Notices Roy. Astron.Soc. **197**, 921.
King, C.R. Ellis, R.S. : 1985, Astrophys. J. **288**, 456.
Kotanyi, C.G., Ekers, R.D. : 1979, Astron. Astrophys. **73**, L1.
Kundt, W., Gopal-Krishna : 1981, Astrophys. Sp.Sci. **75**, 257.
Kundt, W., Krause, M. : 1985, Astron. Astrophys. **142**, 150.
Laing, R.A.: 1981, Monthly Notices Roy. Astron. Soc. **195**, 261.
Laing, R.A. : 1988, Nature **331**, 149.
Laing, R.A. Riley, J.M., Longair, M.S. : 1983, Monthly Notices Roy. Astron. Soc. **204**, 151.
Lang, K.R., 1978, Astrophysical Formulae, p 602, Springer-Verlag.

Large, M.I., Mills, B.Y., Little, A.G., Crawford, D.F., Sutton, J.M. : 1981, Monthly Notices Roy. Astron. Soc. **194**, 693.
Leahy, J.P., Williams, A.G. : 1984, Monthly Notices Roy. Astron. Soc. **210**, 929.
Longair, M.S. : 1966, Monthly Notices Roy. Astron. Soc. **133**, 421.
Longair, M.S., Ryle, M., Scheuer, P.A.G. : 1973, Monthly Notices Roy. Astron. Soc. **164**, 243.
Longair, M.S., Seldner, M. : 1979, Monthly Notices Roy. Astron. Soc. **189**, 433.
Lonsdale, C.J., Barthel, P.D. : 1984, Astron. Astrophys. **135**, 45.
MacDonald, G.H., Kanderdine, S., Neville, A.C. : 1968, Monthly Notices Roy. Astron. Soc.**13**, 259.
MacGillivray, H.I., Stobie, R.S. : 1984, Vistas Astr. **27**, 433.
Machalski, J., Condon, J.J. : 1985, Astron. J. **90**, 973.
Mackay, C.D. : 1969, Monthly Notices Roy. Astron. Soc. **145**, 31.
Macklin, J.T. : 1981. Monthl Notices Roy. Astron. Soc. **196**, 967.
Malin, D.F. : 1977, Am. Astron. Soc. Photogr. Bull No. **16**, 10.
Malin, D.F. : 1978, Nature **276**, 591.
Malin, D.F., Carter, D. : 1983, Astrophys. J. **274**, 534.
Malin, D.F., Quinn, P.J., Graham, J.A. : 1983, Astrophys, J. **272**, L5.
Maltby, P., Matthews, J.A., Moffet, A.T. : 1963, Astrophys. J. **137**, 153.
Marcelin, M., Boulesteix, J., Courtes, G., Milliard, B. : 1982, Nature **297**, 38.
Marshall, F.J., Clark, G.W. : 1981, Astrophys. J. **245**, 840.
Masson, C.R. : 1979, Monthly Notices Roy. Astron. Soc. **187**, 253.
Mayer, C.J. : 1979, Monthly Notices Roy. Astron. Soc. **186**, 99.
Menon, T.K., Hickson, P. : 1985, Astrophys. J. : **296**, 60.
Miley, G.K. : 1980, Annual Rev. Astron. Astrophys. **18**, 165.
Miley, G.K., Osterbrock, D.E. : 1979, Proc. Astron. Soc. Pac. **91**, 257.
Miller, L. : 1985, Monthly Notices Roy. Astron. Soc. **215**, 773.
Miller, L., Longair, M.S., Fabbiano, G., Trinchieri, G., Elvis, M. : 1985, Monthly Notices Roy. Astron. Soc. **215**, 799.
Moffet, A.T. : 196, in Astrophysics and General Relativity, p 219, eds. Chretien, M., Deser, S., Goldstein, J.
Norman, M.L., Burns, J.O., Sulkanen, M.E. : 1988, Nature **335**, 146.
Norman, M.L., Smarr, L.L., Winkler, K. -H.A. : 1982, Astron. Astrophys. **113**, 285.
Nulsen, P., Stewart, G., Fabian, A.C. : 1984, Monthly Notices Roy. Astron. Soc. **208**, 185.
O'Dea, C.P. : 1985, Astrophys. J. **295**, 80.
Oort, M.J.A., Katgert, P., Steeman, F.W.H., Windhorst, R.A. : 1987a, Astron. Astrophys. **179**, 41.
Oort, M.J.A., Katgert, P., Windhorst, R.A. : 1987b, Nature 328, 500.
Osmer, P.S. : 1978, Astrophys. J. **226**, L79.
Owen, F.N., Porcas, R.W., Neff, S.G. : 1978, Astron. J. **83**, 1009.
Parma, P., de Ruiter, H.R., Fanti, C., Fanti, R. : 1986, Astron. Astrophys. Suppl. **64**, 135.
Peacock, J.A. : 1987, in Astrophysical Jets and their Engines, NATO ASI Series **208**, p 171, ed. Kundt, W.
Pence, W.D. : 1986, IAU Symp. **127**, p 463.
Perley, R.A., Bridle, A.H., Willis, A.G. : 1984, Astrophys. J. Suppl. **54**, 291.
Peterson, B.A., Dickens, R.J., Cannon, R.D. : 1975, Proc. Astron. Soc. Aust. **2**, 366.
Phillips, R.D., Mutel, R.L. : 1980, Atrophys. J. **236**, 89.
Prestage, R., Peacock, J.A. : 1988, Monthly Notices Roy. Astron. Soc. **230**, 131.
Purvis, A., Tappin, S.J., Rees, W.G., Hewish, A., Duffet-Smith, P.J. 1987, Monthly Notices Roy. Astron. Soc. **229**, 589.
Quinn, P.J. : 1982, Ph.D. Thesis, Univ. of Canberra.
Quinn, P.J. : 1984, Astrophys. J. **279**, 596.
Rawlings, S., Saunders, R. : 1988, Monthly Notices Roy. Astron. Soc. (in press).
Rana, N.C., Wilkinson, D.A. : 1987, Monthly Notices Roy. Astron. Soc. **226**, 395.
Readhead, A.C.S., Hewish, A. : 1974, Mem. Roy. Astron. Soc. **78**
Readhead, A.C.S., Napier, P.J., Bignell, R.C. : 1980, Astrophys.J. **237**, L55.
Rees, M.J. : 1971, Nature **229**, 312.
Rees, M.J., Setti, G. : 1968, Nature **219**, 127.
Reynolds, J.E. : 1987, in NRAO workshop on Continuum Radio Processes in Clusters of Galaxies, p 59, eds., O'Dea, C.P., Uson, J.M.

Riley, J.M., Pooley, G.G. : 1975, Mem. Roy. Astron. Soc. **80**, 105.
Roland, J. : 1982, Astron. Astrophys. **107**, 267.
Rosen, A., Wiita, P.J. : 1988, Astrophys. J. **330**, 16.
Rudnick, L., Edgar, B.K. : 1984, Astropys. J. **279**, 74.
Ryle, M., Longair, M.S. : 1967, Monthly Notices Roy. Astron. Soc. **136**, 123.
Sandage, A. : 1973, Astrophys. J. **183**, 711.
Saripalli, L., Gopal-Krishna : 1985, Astron. Astrophys. **149**, 205.
Saripalli, L., Gopal-Krishna : 1987, in Astrophysical Jets and their Engines, p 247, ed. Kundt, W.
Saripalli, L., Gopal-Krishna, Reich.W., Kuhr, H. : 1986, Astron. Astrophys. **170**, 20.
Saunders, R. : 1982, Ph.D. Thesis, University of Cambridge
Saunders, R., Baldwin, J.E., Pooley, G.G., Warner, P.J. : 1981, Monthly Notices Roy. Astron. Soc. **197**, 253.
Saunders, R., Baldwin, J.E., Warner, P.J. : 1987, Monthly Notices Roy. Astron. Soc. **225**, 713.
Scheuer, P.A.G. : 1974, Monthly Notices Roy. Astron. Soc. **166**, 513.
Scheuer, P.A.G. : 1977, Radio Astronomy and Cosmology, IAU Symp. **74**, p 343.
Scheuer, P.A.G. : 1982, in Extragalactic Radio Sources, IAU Symp. **97**, p 163.
Scheuer, P.A.G. : 1987, in Astrophysical Jets and their Engines, NATO ASI Series **208**, p 129, ed. Kundt, W.
Schilizzi, R.T., Kapahi, V.K. Neff. .G. : 1982, J. Astron. Astrophys. **3**, 173.
Schilizzi, R.T., McAdam, W.B. : 1975, Men. Roy. Astron. Soc. **79**, 1.
Schreier, E.J., Burns, J.O., Feigelson, E.D. : 1981, Astrophys. J. **251**, 523.
Schreier, E.J., Gorenstein, P.X., Feigelson, E.D. : 1982, Astrophys. J. **261**, 42.
Schwartz, U.J., Whiteoak, J.B., Cole, D.J. : 1973, Aust. J. Phys. **27**, 563.
Schweizer, F. : 1980, Astrophys. J. **237**, 303.
Schweizer, F., Seitzer, P. : 1988, Astrophys. J. **328**, 88.
Scott, M.A. : 1977, Monthly Notices Roy. Astron. Soc. **179**, 377.
Scott, M.A., Readhead, A.C.S. : 1977, Monthly Notices Roy. Astron. Soc. **180**, 539.
Seldner, M., Peebles, P.J.E. : 1978, Astrophys. J. **225**, 7.
Seldner, M., Siebers, B., Groth, E.J., Peebles, P.J.E. : 1977, Astron. J. **82**, 249.
Simon, A.J.B. : 1977, Monthly Notices Roy. Astron. Soc. **178**, 329.
Singal, A.K. : 1988, Monthly Notices Roy. Astron. Soc. **233**, 87.
Slee, O.B., Sheridan, K.V., Dulk, G.A., Little, A.G. : 1983, Proc. Astron. Aust. **5**, 247.
Smith, H.E., Spinrad, H. : 1980, Proc. Astron. Soc. Pac. **92**, 553.
Spangler, S.R. : 1980, Astron. J. **84**, 1470.
Sparks, W.B., Disney, M.J., Wall, J.V., Rodgers, J.W. : 1984, Monthly Notices Roy. Astron. Soc. **207**, 445.
Stocke, J.T. : 1979, Astrophys. J. **230**, 40.
Stockton, A., MacEnty, J.W. : 1987, Astrophys. J. **316**, 584.
Strom, R.G., Baker, J.R., Willis, A.G. : 1981, Astron. Astrophys. **100**, 220.
Strom, R.G., Jagers, W.J. : 1988, Astron. Astrophys. **194**, 79.
Strom, R.G., Willis, A.G. : 1980, Astron. Astrophys. **85**, 36.
Strom, R.G., Willis, A.G., Wilson, A.S. : 1978, Astron.Astrophys. **68**, 367.
Subrahmanya, C.R., Hunstead, R.W. : 1986, Astron. Astrophys, **170**, 27.
Swarup, G. : 1985, J.Astron.Astrophys. **5**, 139.
Swarup, G., Banhatti, D.G. : 1981, Monthly Notices Roy. Astron. Soc. **194**, 1025.
Swarup, G., Bhandari, S.M. : 1974, Astrophys. Lett. **17**, 31.
Swarup, G., et al. : 1971, Nature Phys. Sci **230**, 185.
Swarup, G., Sinha, R.P., Hilldrup, K. : 1984, Monthly Notices Roy. Astron. Soc. **208**, 813.
Tsien, S.C. : 1982, Monthly Notices Roy. Astron. Soc. **200**, 377.
Ulrich,M.-H., Meier, D.L. : 1984, Astron. J. **89**, 203.
Umemura, M., Ikeuchi, S. : 1987, Astrophys. J. **319**, 601.

Valtaoja, E. : 1984, Astron. Astrophys. **140**, 148.
van Breugel, W., et al. :1983, Astrophys. J. **275**, 61.
van Breugel, W., Heckman, T.M., Miley, G.K., Filippenko, A.V. 1986, Astrophys. J. **311**, 58.
Wardle, J.F.C. : 1977, Nature **269**, 563.
Waggett, P.C., Warner, P.J., Baldwin, J.E. : 1977, Monthly Notices Roy. Astron. Soc. **181**, 465.
White, G.L., McAdam, W.B., Jones, I.G. : 1984, Proc. Astron., Soc. Aust. **5**, 507.
Whitford, A.E. : 1971, Astrophys. J. **169**, 215.
Wiita, P.J. 1985, Phys. Reports **123**, 118.
Williams, R.E., Christiansen, W.A. : 1985, Astrophys. J. **291**, 80.
Willis, A.G., Strom, R.G. : 1978, Astron. Astrophys. **62**, 375.
Willis, A.G., Strom, R.G., Bridle, A.H., Fomalont, E.B. : 1981, Astron. Astrophys. **95**, 250.
Willis, A.G., Strom, R.G., Perley, R.A., Bridle, A.H. : 1982, in Extragalactic Radio Sources, IAU Symp. **97**, p 141, eds. Heeschen, D.S., Wade, C.N.
Willis, A.G., Strom, R.G., Wilson, A.S. : 1974, Nature **250**, 625.
Windhorst, R.A. : 1984, Ph.D. Thesis, University of Leiden.
Wood, K.S., et al. : 1984, Astrophys. J. Suppl. **56**, 507.
Yee, H.K.C., Green, R.E. : 1984, Astrophys. J. **280**, 79.
Yee, H.K.C., Oke, J.B. : 1978, Astrophys. J. **226**, 753.
Young, P.J., Sargent, W.L.W., Kristian, J., Westphal, J.A. : 1979, Astrophys. J. **234**, 76.
Zwicky, F., Herzog, E. : 1963, Catalogue of Galaxies and Clusters of Galaxies, (Cal. Tech.).